

# Chapter 1

## Random tessellations and Cox processes

Florian Voss, Catherine Gloaguen and Volker Schmidt

**Abstract** We consider random tessellations  $T$  in  $\mathbb{R}^2$  and Coxian point processes whose driving measure is concentrated on the edges of  $T$ . In particular, we discuss several classes of Poisson-type tessellations which can describe e.g. the infrastructure of telecommunication networks, whereas the Cox processes on their edges can describe the locations of network components. An important quantity associated with stationary point processes is their typical Voronoi cell  $\mathcal{E}^*$ . Since the distribution of  $\mathcal{E}^*$  is usually unknown, we discuss algorithms for its Monte Carlo simulation. They are used to compute the distribution of the typical Euclidean (i.e. direct) connection length  $D^*$  between pairs of network components. We show that  $D^*$  converges in distribution to a Weibull distribution if the network is scaled and network components are simultaneously thinned in an appropriate way. We also consider the typical shortest path length  $C^*$  to connect network components along the edges of the underlying tessellation. In particular, we explain how scaling limits and analytical approximation formulae can be derived for the distribution of  $C^*$ .

### 1.1 Random tessellations

In the section we introduce the notion of random tessellations in  $\mathbb{R}^2$ , where we show that they can be regarded as marked point processes as well as random closed sets, and we discuss some mean-value formulae of stationary random tessellations. Furthermore, we introduce simple tessellation models of Poisson type like Poisson-Voronoi, Poisson-Delaunay and Poisson line tessellations.

---

Florian Voss and Volker Schmidt  
Ulm University, Institute of Stochastics, Helmholtzstraße 18, D-89069 Ulm, Germany, e-mail:  
volker.schmidt@uni-ulm.de, florian.voss@uni-ulm.de  
Catherine Gloaguen  
Orange Labs, 92131 Issy les Moulineaux Cedex 9, France, e-mail: catherine.gloaguen@orange-ftgroup.com

### 1.1.1 Basis definitions, results and notation

To begin with, we briefly summarize the basic notation and mathematical background from point process theory which we are using throughout this chapter. For more details and further information about these topics and stochastic geometry in general see for example [3, 16, 17] and the other chapters of the present book. Note that we only regard the planar case in the following, although most of the results presented here can be generalized easily to  $\mathbb{R}^d$  for  $d > 2$ .

Let  $\mathbb{N} = \mathbb{N}(\mathbb{R}^2)$  denote the family of simple and locally finite counting measures on the Borel  $\sigma$ -algebra  $\mathcal{B}(\mathbb{R}^2)$ . Then we define the  $\sigma$ -algebra  $\mathcal{N} = \mathcal{N}(\mathbb{R}^2)$  on  $\mathbb{N}$  as the  $\sigma$ -algebra generated by all sets of the form  $\{\varphi \in \mathbb{N} : \varphi(B) = j\}$  with  $j \in \mathbb{N}_0$  and  $B \in \mathcal{B}_0(\mathbb{R}^2)$ , where  $\mathcal{B}_0(\mathbb{R}^2)$  denotes the family of bounded Borel sets. In the following,  $t_x : \mathbb{N} \rightarrow \mathbb{N}$  denotes the shift operator defined by  $t_x\varphi(B) = \varphi(B+x)$  for any  $x \in \mathbb{R}^2$  and  $B \in \mathcal{B}(\mathbb{R}^2)$ . Thus,  $t_x$  translates all atoms of  $\varphi \in \mathbb{N}$  by  $-x$ .

A measurable mapping  $X : \Omega \rightarrow \mathbb{N}$  from some probability space  $(\Omega, \mathcal{A}, \mathbb{P})$  into the measurable space  $(\mathbb{N}, \mathcal{N})$  is called a *random point process* in  $\mathbb{R}^2$ . There are different ways to look at point processes. We interpret  $X = \{X_n\}$  either as a random counting measure using the notation  $X(B)$  for the (random) number of atoms of  $X$  in  $B \in \mathcal{B}(\mathbb{R}^2)$  or as a random (finite or countably infinite) sequence  $X_1, X_2, \dots$  of (2-dimensional) random variables  $X_n : \Omega \rightarrow \mathbb{R}^2$ .

The probability measure  $P_X$  defined on  $\mathcal{N}$  by  $P_X(A) = \mathbb{P}(X \in A)$  for  $A \in \mathcal{N}$  is called the *distribution* of  $X$ . A point process  $X$  is called *stationary* if  $P_X = P_{t_x X}$  for any  $x \in \mathbb{R}^2$ . We define the *intensity measure*  $\mu : \mathcal{B}(\mathbb{R}^2) \rightarrow [0, \infty]$  of a point process  $X$  by  $\mu(B) = \mathbb{E}X(B)$ ,  $B \in \mathcal{B}(\mathbb{R}^2)$ . In the following we will always assume that  $\mu$  is locally finite. If  $X$  is stationary, we additionally assume that  $P(X(\mathbb{R}^2) > 0) = 1$ . Then, for some constant  $\lambda > 0$  which is called the *intensity* of  $X$ , we have  $\mu(B) = \lambda v_2(B)$  for any  $B \in \mathcal{B}(\mathbb{R}^2)$ , where  $v_2$  denotes the 2-dimensional Lebesgue measure.

Point processes can be generalized by adding a (random) mark from some mark space  $\mathbb{M}$  to each point. Such generalizations are called marked point processes. In the following, the *mark space*  $\mathbb{M}$  is assumed to be a Polish space which is equipped with the Borel- $\sigma$ -algebra  $\mathcal{B}(\mathbb{M})$  on  $\mathbb{M}$ . Let  $\mathbb{N}_{\mathbb{M}} = \mathbb{N}(\mathbb{R}^2 \times \mathbb{M})$  denote the set of all measures  $\psi : \mathcal{B}(\mathbb{R}^2) \otimes \mathcal{B}(\mathbb{M}) \rightarrow \mathbb{N}_0 \cup \{\infty\}$  which are simple and locally finite in the first component, i.e.,  $\psi(\{x\} \times \mathbb{M}) \in \{0, 1\}$  for all  $x \in \mathbb{R}^2$  and  $\psi(B \times \mathbb{M}) < \infty$  for all  $B \in \mathcal{B}_0(\mathbb{R}^2)$ . Now let  $\mathcal{N}_{\mathbb{M}}$  be the  $\sigma$ -algebra generated by the subsets of  $\mathbb{N}_{\mathbb{M}}$  of the form  $\{\psi \in \mathbb{N}_{\mathbb{M}} : \psi(B \times G) = j\}$  for  $B \in \mathcal{B}_0(\mathbb{R}^2)$ ,  $G \in \mathcal{B}(\mathbb{M})$  and  $j \in \mathbb{N}_0$ . We then call a measurable mapping  $X_M : \Omega \rightarrow \mathbb{N}_{\mathbb{M}}$  from some probability space  $(\Omega, \mathcal{A}, \mathbb{P})$  into the measurable space  $(\mathbb{N}_{\mathbb{M}}, \mathcal{N}_{\mathbb{M}})$  a *random marked point process* in  $\mathbb{R}^2$  with mark space  $(\mathbb{M}, \mathcal{B}(\mathbb{M}))$ . Again, often alternative representations of  $X_M$  are convenient. For instance,  $X_M$  can be represented as a sequence of random marked points written as  $X_M = \{(X_n, M_n)\}$ . Here both  $X_n : \Omega \rightarrow \mathbb{R}^2$  and  $M_n : \Omega \rightarrow \mathbb{M}$  are measurable mappings. In the following we use the notation  $X_M = \{(X_n, M_n)\}$  and we regard  $X_M$  as a random sequence of marked points or a random element of  $\mathbb{N}_{\mathbb{M}}$ .

The distribution  $P_{X_M}$  of  $X_M$  is given by  $P_{X_M}(A) = \mathbb{P}(X_M \in A)$  for any  $A \in \mathcal{N}_{\mathbb{M}}$ . Stationarity is now defined with respect to the first component of  $X_M$ , where the shift operator  $t_x : \mathbb{N}_{\mathbb{M}} \rightarrow \mathbb{N}_{\mathbb{M}}$  is considered with  $t_x\psi = \{(x_n - x, m_n)\}$  for  $\psi = \{(x_n, m_n)\}$ .

The marked point process  $X_M$  is called *stationary* if  $P_{X_M} = P_{t_x X_M}$  for all  $x \in \mathbb{R}^2$ . Then  $\lambda = \mathbb{E}X_M([0, 1]^2 \times \mathbb{M}) > 0$  is called the *intensity* of  $X_M$  and the probability measure  $P_{X_M}^o : \mathcal{B}(\mathbb{M}) \rightarrow [0, 1]$  defined by

$$P_{X_M}^o(G) = \frac{1}{\lambda} \mathbb{E}\#\{n \in \mathbb{N} : X_n \in [0, 1]^2, D_n \in G\}, \quad G \in \mathcal{B}(\mathbb{M}), \quad (1.1)$$

is called the *Palm mark distribution* of  $X_M$ . A random variable  $M^* : \Omega \rightarrow \mathbb{M}$  distributed according to  $P_{X_M}^o$  is called the *typical mark* of  $X_M$ . It can be interpreted as the conditional distribution of the mark at the origin  $o$  given that there is a point of  $X_M$  located at  $o$ . Moreover, for any stationary marked point process  $X_M$ , the *Palm distribution*  $P_{X_M}^*$  is the probability measure on  $\mathcal{N}_{\mathbb{M}} \otimes \mathcal{B}(\mathbb{M})$  given by

$$P_{X_M}^*(A \times G) = \frac{1}{\lambda} \mathbb{E}\#\{n \in \mathbb{N} : X_n \in [0, 1]^2, M_n \in G, t_{X_n} X_M \in A\} \quad (1.2)$$

for  $A \in \mathcal{N}_{\mathbb{M}}$ ,  $G \in \mathcal{B}(\mathbb{M})$ . It can be interpreted as conditional distribution of  $X_M$  under the condition that there is a point of  $X_M$  at  $o$ . A marked point process with distribution  $P_{X_M}^*(\cdot \times \mathbb{M})$  is denoted by  $X_M^*$  and called the *Palm version* of  $X_M$ . The next result is called the *refined Campbell theorem*, see e.g. Theorem 3.5.3 in [16].

**Theorem 1.** *Let  $X_M$  be a stationary marked point process in  $\mathbb{R}^2$  with mark space  $\mathbb{M}$  and intensity  $\lambda > 0$ . Furthermore, let  $f : \mathbb{R}^2 \times \mathbb{M} \times \mathbb{N}_{\mathbb{M}} \rightarrow [0, \infty)$  be measurable. Then  $\sum_{(x,m) \in X_M} f(x, m, t_x X_M)$  is a well-defined random variable and*

$$\mathbf{E} \sum_{(x,m) \in X_M} f(x, m, t_x X_M) = \lambda \int_{\mathbb{R}^2} \int_{\mathbb{N}_{\mathbb{M}} \times \mathbb{M}} f(x, m, \psi) P_{X_M}^*(d(\psi, m)) \nu_2(dx). \quad (1.3)$$

Ergodic and mixing marked point processes are defined in the following way. We define the shift  $t_x A$  of a set  $A \in \mathcal{N}_{\mathbb{M}}$  by  $t_x A = \{t_x \psi : \psi \in A\}$  for all  $x \in \mathbb{R}^2$ . Then, a stationary marked point process  $X_M$  is called *ergodic* if  $\mathbb{P}(X_M \in A) \in \{0, 1\}$  for all  $A \in \mathcal{I}$ , where  $\mathcal{I} = \{A \in \mathcal{N}_{\mathbb{M}} : A = t_x A \text{ for all } x \in \mathbb{R}^2\}$  denotes the  $\sigma$ -algebra of shift invariant sets in  $\mathcal{N}_{\mathbb{M}}$ . A stationary marked point process  $X_M$  is called *mixing* if  $\lim_{|x| \rightarrow \infty} \mathbb{P}(X_M \in A, X_M \in t_x B) = \mathbb{P}(X_M \in A) \mathbb{P}(X_M \in B)$  for  $A, B \in \mathcal{N}_{\mathbb{M}}$ . If  $A \in \mathcal{I}$  and  $X$  is mixing, then  $\mathbb{P}(X \in A) = \lim_{|x| \rightarrow \infty} \mathbb{P}(X \in A, X \in t_x A) = \mathbb{P}(X \in A) \mathbb{P}(X \in A) = \mathbb{P}(X \in A)^2$ . This shows that  $X$  is ergodic if  $X$  is mixing.

We now state still another basic result which is a version of the individual and statistical ergodic theorem applied to marked point processes, see Theorem 12.2.IV and Corollary 12.2.V in [3]. It connects spatial averages of the marks of an ergodic marked point process with statistical averages of the typical mark.

**Theorem 2.** *Let  $X_M$  be an ergodic marked point process with intensity  $\lambda$  and mark space  $\mathbb{M}$ , and let  $M^*$  be the typical mark of  $X_M$ . Then, for any convex averaging sequence  $\{W_n\}_{n \geq 1}$  and for any measurable function  $h : \mathbb{M} \rightarrow [0, \infty)$ , it holds that*

$$\mathbf{E}h(M^*) = \lim_{n \rightarrow \infty} \frac{1}{\lambda \nu_2(W_n)} \sum_{i=1}^{\infty} \mathbf{1}_{W_n}(X_i) h(M_i) \quad (1.4)$$

almost surely and in  $L^1$ . Furthermore, with probability 1, it holds that

$$\mathbf{E}h(M^*) = \lim_{n \rightarrow \infty} \frac{1}{\#\{i : X_i \in W_n\}} \sum_{i=1}^{\infty} \mathbf{1}_{W_n}(X_i) h(M_i). \quad (1.5)$$

By the result of Theorem 2 it becomes clear why we are interested in the typical mark of ergodic marked point processes: For  $h = \mathbf{1}_G$ , formula (1.5) implies that

$$P_{X_M}^o(G) = \lim_{n \rightarrow \infty} \frac{\#\{i \in \mathbb{N}_0 : X_i \in [-n, n]^2, M_i \in G\}}{X_M([-n, n]^2 \times \mathbb{M})}. \quad (1.6)$$

Thus, the typical mark can be seen as the mark at a point chosen at random among all points, i.e., at the typical point of the “unmarked” point process  $\{X_n\}$ .

### 1.1.2 Deterministic tessellations

Intuitively speaking, a tessellation is a subdivision of  $\mathbb{R}^2$  into a sequence of convex polygons. However, a tessellation can also be identified with the segment system consisting of the boundaries of these polygons. Because of these different viewpoints, random tessellations introduced later on in Section 1.1.3 are flexible models which can be applied in many different fields of science.

We start with the definition of deterministic planar tessellations. A *tessellation*  $\tau$  in  $\mathbb{R}^2$  is a countable family  $\{\xi_n\}_{n \geq 1}$  of convex bodies  $\xi_n$  fulfilling the conditions  $\xi_n \neq \emptyset$  for all  $n$ ,  $\xi_n \cap \xi_m = \emptyset$  for all  $n \neq m$ ,  $\bigcup_{n \geq 1} \xi_n = \mathbb{R}^2$  and  $\sum_{n \geq 1} \mathbf{1}_{\{\xi_n \cap C \neq \emptyset\}} < \infty$  for any  $C \in \mathcal{C}$ , where  $\overset{\circ}{\xi}$  denotes the interior of the set  $\xi \subset \mathbb{R}^2$ , and  $\mathcal{C}$  is the family of compact sets in  $\mathbb{R}^2$ . The sets  $\xi_n$  are called the *cells* of the tessellation  $\tau$  and are bounded polygons in  $\mathbb{R}^2$ . In the following, we use the notation  $\mathbb{T}$  for the family of all tessellations in  $\mathbb{R}^2$ . Note that we can identify a tessellation  $\tau$  with the segment system  $\tau^{(1)} = \bigcup_{n=1}^{\infty} \partial \xi_n$  constructed from the boundaries of the cells of  $\tau$ . Thus, a tessellation can be identified with a closed subset of  $\mathbb{R}^2$  and hence we can regard  $\mathbb{T}$  as a subset of the family  $\mathcal{F}$  of all closed subsets of  $\mathbb{R}^2$ . We use this connection in order to define the  $\sigma$ -algebra  $\mathcal{T}$  on  $\mathbb{T}$  as the trace- $\sigma$ -algebra of  $\mathcal{B}(\mathcal{F})$  in  $\mathbb{T}$ .

With each cell  $\xi_n$  of  $\tau$  we can associate some “marker point” in the following way. Consider a mapping  $\alpha : \mathcal{C} \setminus \{\emptyset\} \rightarrow \mathbb{R}^2$  which satisfies

$$\alpha(\xi + x) = \alpha(\xi) + x \quad \text{for all } \xi \in \mathcal{C}, \xi \neq \emptyset \text{ and } x \in \mathbb{R}^2, \quad (1.7)$$

where  $\alpha(\xi)$  is called the *nucleus* of  $\xi$  and can be e.g. the center of gravity of  $\xi$ .

There are various ways to generate tessellations based on sets of points and lines. Particular models are Voronoi tessellations and Delaunay tessellations as well as line tessellations which are introduced in the following.

Let  $\mathbf{x} = \{x_1, x_2, \dots\} \subset \mathbb{R}^2$  be a locally finite set with  $\text{conv}(\mathbf{x}) = \mathbb{R}^2$ , where  $\text{conv}(\mathbf{x})$  denotes the convex hull of the family  $\mathbf{x}$ . Then the *Voronoi tessellation*  $\tau$  induced by

$\mathbf{x}$  is defined by the nearest-neighbor principle, i.e., the cells  $\xi_n$  of  $\tau$  are given by

$$\xi_n = \{x \in \mathbb{R}^2 : |x - x_n| \leq |x - x_m| \text{ for all } m \neq n\}. \quad (1.8)$$

Note that  $\xi_n = \bigcap_{m \neq n} H(x_n, x_m)$ , i.e. the cell  $\xi_n$  can be represented as intersection of the half-planes  $H(x_n, x_m) = \{x \in \mathbb{R}^2 : |x - x_n| \leq |x - x_m|\}$  for  $m \neq n$ , where the half-planes  $H(x_n, x_m)$  are also called *bisectors*. Since  $\mathbf{x}$  is locally finite it is clear that the cells of  $\tau$  have non-empty interior. Moreover, their union covers  $\mathbb{R}^2$  and two different cells can only intersect at their boundaries. Using that  $\text{conv}(\mathbf{x}) = \mathbb{R}^2$ , it can be shown that the cells are convex polygons which are bounded and locally finite. Thus, the family  $\tau = \{\xi_n\}$  constructed in this way is indeed a tessellation. A Voronoi tessellation together with the generating point set is displayed in Figure 1.1(a).

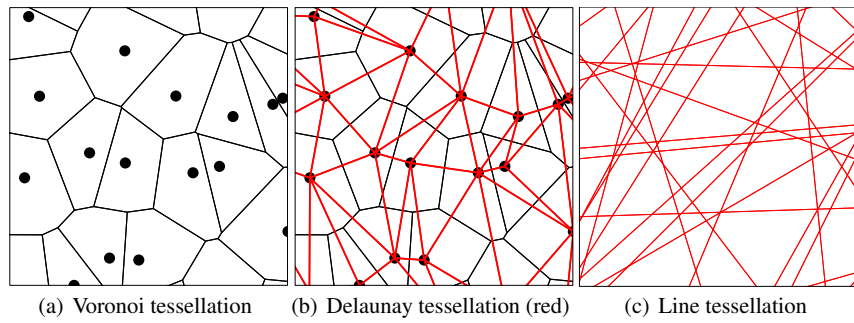


**Fig. 1.1** Different types of tessellation models

Now assume that four cocircular points do not exist in  $\mathbf{x}$ , i.e., we assume that there are no pairwise different points  $x_i, x_j, x_k, x_l \in \mathbf{x}$  which are located on a circle. In this case, the *Delaunay tessellation*  $\tau'$  induced by  $\mathbf{x}$  can be generated uniquely as the dual tessellation of the Voronoi tessellation  $\tau$  which is induced by  $\mathbf{x}$ . The cells of  $\tau'$  are triangles which are constructed in the following way. Three points  $x_i, x_j, x_k \in \mathbf{x}$  form a triangle of  $\tau'$  if the corresponding Voronoi cells  $\xi_i, \xi_j$  and  $\xi_k$  have a common intersection point. This rule is equivalent to the empty circle criterion: three points of  $\mathbf{x}$  are the vertices of a triangle of  $\tau'$  if and only if the circumcircle of these three points does not contain other points of  $\mathbf{x}$ . It can be shown that the resulting sequence of triangles forms a tessellation in  $\mathbb{R}^2$ . In Figure 1.1(b) a Delaunay tessellation is displayed together with its generating points and the dual Voronoi tessellation.

Consider a set  $\ell = \{\ell_1, \ell_2, \dots\}$  of lines in  $\mathbb{R}^2$  and let  $p_i \in \mathbb{R}^2$  denote the orthogonal projection of  $o$  onto  $\ell_i$ , where it is assumed that  $\text{conv}(\{p_1, p_2, \dots\}) = \mathbb{R}^2$ . Furthermore, we assume that  $\#\{i : \ell_i \cap B \neq \emptyset\} < \infty$  for all  $B \in \mathcal{C}$ . Then, in a natural way, we can generate a tessellation with respect to the intersecting lines of  $\ell$ . Recall that we can identify a tessellation  $\tau$  with the edge set  $\tau^{(1)} = \bigcup_{n=1}^{\infty} \partial \xi_n$  given by the union of the cell boundaries. Thus, we define the *line tessellation*  $\tau$  induced by  $\ell$  via the edge set  $\tau^{(1)} = \bigcup_{i=1}^{\infty} \ell_i$  formed by the union of the lines  $\ell_1, \ell_2, \dots$ . If the family  $\ell$

fulfills the assumptions above, then it is ensured that the resulting cells possess the properties of a tessellation of  $\mathbb{R}^2$ , see also Figure 1.1(c).

### 1.1.3 Random tessellations

Usually, a *random tessellation* in  $\mathbb{R}^2$  is defined as a measurable mapping  $T : \Omega \rightarrow \mathbb{T}$ , i.e. as a sequence  $T = \{\mathcal{E}_n\}$  of random convex bodies  $\mathcal{E}_n$  such that  $\mathbb{P}(\{\mathcal{E}_n\} \in \mathbb{T}) = 1$ . Notice that there are various ways to look at tessellations. In particular, they can be viewed as marked point processes and random closed sets. Each of these different points of view leads to new characteristics that can be associated with a tessellation. The tessellation  $T$  is said to be stationary and isotropic if  $t_x T = \{t_x \mathcal{E}_n\} \stackrel{d}{=} T$  for all  $x \in \mathbb{R}^2$  and  $\vartheta_R T = \{\vartheta_R \mathcal{E}_n\} \stackrel{d}{=} T$  for all rotations  $\vartheta_R$  around the origin, respectively.

#### 1.1.3.1 Random tessellations as marked point processes

It is often convenient to represent a random tessellation  $T = \{\mathcal{E}_n\}$  as a marked point process with an appropriate mark space. Note that we can associate various point processes with  $T$ , e.g. the point processes of cell nuclei, vertices and edge midpoints. If these point processes are marked with suitable marks, then we can identify  $T$  with the corresponding marked point process.

We first consider the *point process of cell nuclei* marked with the cells. Let  $\alpha : \mathcal{C} \setminus \{\emptyset\} \rightarrow \mathbb{R}^2$  be a mapping such that (1.7) holds. Let  $\mathcal{P}^o$  denote the family of all convex and compact polygons  $\xi$  with their nucleus  $\alpha(\xi)$  at the origin. Then  $\mathcal{P}^o \subset \mathcal{F}$  is an element of  $\mathcal{B}(\mathcal{F})$  and we can define the  $\sigma$ -algebra  $\mathcal{B}(\mathcal{P}^o) = \mathcal{B}(\mathcal{F}) \cap \mathcal{P}^o$ . Furthermore, the random tessellation  $T = \{\mathcal{E}_n\}$  can be identified with the marked point process  $\{(\alpha(\mathcal{E}_n), \mathcal{E}_n^o)\}$ , where  $\mathcal{E}_n^o = \mathcal{E}_n - \alpha(\mathcal{E}_n)$  is the  $n$ -th cell shifted to the origin. If  $T$  is stationary, then  $\{(\alpha(\mathcal{E}_n), \mathcal{E}_n^o)\}$  is also stationary and we denote its intensity by  $\lambda^{(2)}$ , where we always assume that  $0 < \lambda^{(2)} < \infty$ . The typical mark  $\mathcal{E}^* : \Omega \rightarrow \mathcal{P}^o$  of  $\{(\alpha(\mathcal{E}_n), \mathcal{E}_n^o)\}$  is a random polygon distributed according to the Palm mark distribution of  $\{(\alpha(\mathcal{E}_n), \mathcal{E}_n^o)\}$  as defined in (1.1). We call the random polygon  $\mathcal{E}^*$  the *typical cell* of the tessellation  $T$ , see also CALKA and HUG.

Another possibility to represent  $T$  by a marked point process is the following. Consider the *point process of vertices*  $V = \{V_n\}$  of  $T$ . For each vertex  $V_n$  we define the *edge star*  $E_n$  as the union of all edges of  $T$  emanating from  $V_n$ . Thus,  $E_n^o = E_n - V_n$  is an element of the family  $\mathcal{L}^o$  of finite segment systems containing the origin. Since  $\mathcal{L}^o \in \mathcal{B}(\mathcal{F})$  we can consider the  $\sigma$ -algebra  $\mathcal{B}(\mathcal{L}^o) = \mathcal{B}(\mathcal{F}) \cap \mathcal{L}^o$  on  $\mathcal{L}^o$ . Hence, we can represent the random tessellation  $T$  by the marked point process  $\{(V_n, E_n^o)\}$  with mark space  $\mathcal{L}^o$ . If  $T$  is stationary, then  $\{(V_n, E_n^o)\}$  is stationary and its intensity is denoted by  $\lambda^{(0)}$ , where we assume that  $0 < \lambda^{(0)} < \infty$ . The *typical edge star*  $E^* : \Omega \rightarrow \mathcal{L}^o$  of  $T$  is defined as a random segment system distributed according to the Palm mark distribution of  $\{(V_n, E_n^o)\}$ .

The random tessellation  $T$  can also be represented by the marked *point process of edge midpoints*  $\{(Y_n, S_n^0)\}$ , where each midpoint  $Y_n$  is marked with the centered version  $S_n^0 = S_n - Y_n \in \mathcal{L}^o$  of the edge  $S_n$  corresponding to  $Y_n$ . If  $T$  is stationary, then it is easy to see that  $\{(Y_n, S_n^0)\}$  is stationary. The intensity of edge midpoints is denoted by  $\lambda^{(1)}$ , where we again assume that  $0 < \lambda^{(1)} < \infty$ . The *typical edge*  $S^* : \Omega \rightarrow \mathcal{L}^o$  is defined as the typical mark of the stationary marked point process  $\{(Y_n, S_n^0)\}$ .

### 1.1.3.2 Random tessellations as random closed sets

In the preceding section random tessellations have been represented as marked point processes. Alternatively, random tessellations can be regarded as random closed sets, see MOLCHANOV for their definition and basic properties. Recall that deterministic tessellations can be identified with their edge sets. Thus, in the random setting, we can identify a random tessellation  $T = \{\mathcal{E}_n\}$  with the corresponding *random closed set* of its edges which is defined by  $T^{(1)} = \cup_{n=1}^{\infty} \partial \mathcal{E}_n$ . If  $T$  is stationary and isotropic, then the random closed set  $T^{(1)}$  is stationary and isotropic, respectively. Since, almost surely,  $T^{(1)}$  is a locally finite system of line segments, we can consider the 1-dimensional Hausdorff measure  $\nu_1$  on  $T^{(1)}$ . Furthermore, if  $T$  is stationary, then it is not difficult to see that  $\mathbf{E}\nu_1(B \cap T^{(1)}) = \gamma \nu_2(B)$  for any  $B \in \mathcal{B}(\mathbb{R}^2)$  and some constant  $\gamma$  which is called the *length intensity* of  $T^{(1)}$ . As for the intensities  $\lambda^{(0)}, \lambda^{(1)}$  and  $\lambda^{(2)}$  regarded above, we always assume that  $0 < \gamma < \infty$ .

### 1.1.3.3 Mean-value formulae

We now discuss mean-value formulae for stationary tessellations. These are relationships connecting the intensities of vertices  $\lambda^{(0)}$ , edge midpoints  $\lambda^{(1)}$  and cell nuclei  $\lambda^{(2)}$ , the length intensity  $\gamma = \mathbf{E}\nu_1(T^{(1)} \cap [0, 1]^2)$ , the expected area  $\mathbf{E}\nu_2(\mathcal{E}^*)$ , perimeter  $\mathbf{E}\nu_1(\partial \mathcal{E}^*)$  and number of vertices  $\mathbf{E}\nu_0(\mathcal{E}^*)$  of the typical cell  $\mathcal{E}^*$ , the expected length of the typical edge  $\mathbf{E}\nu_1(S^*)$ , and the expected length  $\mathbf{E}\nu_1(E^*)$  and number of edges  $\mathbf{E}\nu_0(E^*)$  of the typical edge star  $E^*$ . It turns out that all these characteristics can be expressed by e.g. the three parameters  $\lambda^{(0)}, \lambda^{(2)}$  and  $\gamma$ .

**Theorem 3.** *It holds that*

$$\begin{aligned} \lambda^{(1)} &= \lambda^{(0)} + \lambda^{(2)}, & \mathbf{E}\nu_0(E^*) &= 2 + 2\frac{\lambda^{(2)}}{\lambda^{(0)}}, & \mathbf{E}\nu_1(E^*) &= 2\frac{\lambda^{(1)}}{\lambda^{(0)}}\mathbf{E}\nu_1(S^*), \\ \mathbf{E}\nu_0(\mathcal{E}^*) &= 2 + 2\frac{\lambda^{(0)}}{\lambda^{(2)}}, & \mathbf{E}\nu_2(\mathcal{E}^*) &= \frac{1}{\lambda^{(2)}}, & \mathbf{E}\nu_1(\partial \mathcal{E}^*) &= 2\frac{\lambda^{(1)}}{\lambda^{(2)}}\mathbf{E}\nu_1(S^*), \\ \gamma &= \lambda^{(1)}\mathbf{E}\nu_1(S^*) = \frac{\lambda^{(2)}}{2}\mathbf{E}\nu_1(\partial \mathcal{E}^*), & & & 3 \leq \mathbf{E}\nu_0(\mathcal{E}^*), \mathbf{E}\nu_0(E^*) &\leq 6. \end{aligned}$$

*Proof.* We show how some of the formulae stated above can be proven using Campbell's theorem for stationary marked point processes; see Theorem 1. For example, consider the marked point process  $\{(Y_n, S_n^0)\}$  of edge midpoints  $Y_n$  marked with the

centered edges  $S_n^o$ . Then, Theorem 1 yields

$$\begin{aligned}
\gamma &= \mathbf{E}v_1(T^{(1)} \cap [0, 1]^2) = \mathbf{E} \sum_{n=1}^{\infty} v_1(S_n^o + Y_n \cap [0, 1]^2) \\
&= \lambda^{(1)} \int_{\mathbb{R}^2} \mathbf{E} \underbrace{v_1(S^* \cap [0, 1]^2 - x)}_{= \int_{S^*} \mathbf{1}_{[0, 1]^2 - x}(y) v_1(dy)} v_2(dx) \\
&= \lambda^{(1)} \mathbf{E} \int_{S^*} \int_{\mathbb{R}^2} \mathbf{1}_{[0, 1]^2 - y}(x) v_2(dx) v_1(dy) = \lambda^{(1)} \mathbf{E}v_1(S^*),
\end{aligned}$$

thus  $\gamma = \lambda^{(1)} \mathbf{E}v_1(S^*)$ . Furthermore,

$$\begin{aligned}
\lambda^{(2)} \mathbf{E}v_2(\mathcal{E}^*) &= \lambda^{(2)} \mathbf{E} \int_{\mathbb{R}^2} \mathbf{1}_{\mathcal{E}^*}(-x) v_2(dx) \\
&= \mathbf{E} \sum_{(\alpha(\mathcal{E}_n), \mathcal{E}_n^o) \in T} \underbrace{\mathbf{1}_{\mathcal{E}_n^o}(-\alpha(\mathcal{E}_n))}_{= \mathbf{1}_{\mathcal{E}_n}(o)} = 1,
\end{aligned}$$

which yields  $\mathbf{E}v_2(\mathcal{E}^*) = 1/\lambda^{(2)}$ . The other statements can be proven similarly. For a complete proof of Theorem 3, see e.g. [2, 13].  $\square$

### 1.1.4 Tessellation models of Poisson type

In this section we consider several tessellation models of Poisson type, like Poisson-Voronoi, Poisson-Delaunay and Poisson line tessellations. They are based on planar or linear Poisson point processes, where a point process  $X = \{X_n\}$  in  $\mathbb{R}^2$  with intensity measure  $\mu$  is called a *Poisson process* if the random variables  $X(B) = \#\{n \in \mathbb{N} : X_n \in B\}$  are Poisson-distributed with  $X(B) \sim \text{Poi}(\mu(B))$  for each  $B \in \mathcal{B}_0(\mathbb{R}^2)$  and if  $X(B_1), \dots, X(B_k)$  are independent for any pairwise disjoint sets  $B_1, \dots, B_k \in \mathcal{B}_0(\mathbb{R}^2)$ . Note that Poisson processes on the real line are defined in the same way.

#### 1.1.4.1 Poisson-Voronoi tessellation

In Section 1.1.2 the notion of a deterministic Voronoi tessellation has been introduced for a certain class of locally finite point sets. Since almost every realization of a stationary point process  $X = \{X_n\}$  with  $\mathbb{P}(X(\mathbb{R}^2) = \infty) = 1$  is a locally finite point set such that  $\text{conv}(X) = \mathbb{R}^2$ , we can regard the random Voronoi tessellation  $\{\mathcal{E}_n\}$  with respect to the point process  $\{X_n\}$ . Thus, in accordance with (1.8), the cells  $\mathcal{E}_n$  are defined as the random closed sets  $\mathcal{E}_n = \{x \in \mathbb{R}^2 : |x - X_n| \leq |x - X_m| \forall m \neq n\}$ . We call  $T = \{\mathcal{E}_n\}$  the Voronoi tessellation induced by  $X$ . Note that we can consider the point  $X_n$  as nucleus of the cell  $\mathcal{E}_n$ . If the underlying point process  $X$  is stationary,

then the Voronoi tessellation induced by  $X$  is also stationary. In particular, if  $X$  is a stationary Poisson process with intensity  $\lambda > 0$ , then we call the induced Voronoi tessellation a *Poisson–Voronoi tessellation* (PVT). Realizations of PVT are shown in Figures 1.2 and 1.3(a). Note that  $v_0(E_n) = 3$  for all  $n \in \mathbb{N}$ ,  $\lambda^{(0)} = \lambda$ , and the intensities  $\lambda^{(1)}$ ,  $\lambda^{(2)}$  and  $\gamma$  can be computed in the following way.

**Theorem 4.** *Let  $T$  be a PVT induced by a Poisson process with intensity  $\lambda$ . Then*

$$\lambda^{(0)} = 2\lambda, \quad \lambda^{(1)} = 3\lambda, \quad \lambda^{(2)} = \lambda, \quad \gamma = 2\sqrt{\lambda}.$$

*Proof.* Applying Theorem 3 with  $\lambda^{(2)} = \lambda$  and  $\mathbf{E}v_0(E^*) = 3$  yields  $\lambda^{(0)} = 2\lambda$ ,  $\lambda^{(1)} = 3\lambda$ , and  $\lambda^{(2)} = \lambda$ . For the proof of  $\gamma = 2\sqrt{\lambda}$  see e.g. [16], Chapter 10.  $\square$

Consider the random Voronoi tessellation  $T$  induced by any stationary (not necessarily Poisson) point process  $X$ . Then, the distribution of the typical cell of  $T$  is given by the distribution of the Voronoi cell at  $o$  with respect to the Palm version  $X^*$  of  $X$ . In particular, due to Slivnyak’s theorem for stationary Poisson processes (see e.g. [16]), we get that the typical cell of a PVT is obtained as the Voronoi cell at  $o$  with respect to the point process  $X^* = X \cup \{o\}$ , see Figure 1.2(b).

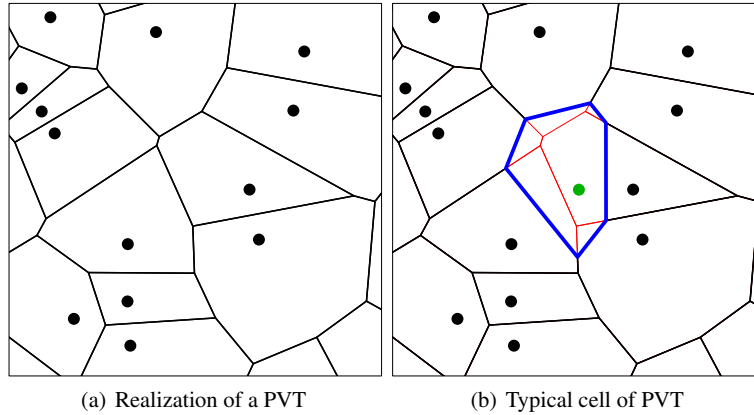


**Fig. 1.2** Realization of a PVT and its typical cell

### 1.1.4.2 Poisson–Delaunay tessellation

In the same way as in Section 1.1.2 for deterministic Voronoi tessellations, we can construct the dual Delaunay tessellation corresponding to a random Voronoi tessellation. If, almost surely, the underlying point process  $X$  is locally finite, where  $\text{conv}(X) = \mathbb{R}^2$  and no four points of  $X$  are cocircular, then the random Delaunay tessellation  $T$  induced by  $X$  is well-defined. Furthermore,  $T$  is stationary if  $X$  is stationary. In particular, if  $X$  is a stationary Poisson process with intensity  $\lambda > 0$ , we

can generate the Delaunay tessellation  $T = \{\Xi_n\}$  of  $X$  as the dual tessellation of the PVT induced by  $X$ , where  $T$  is called a *Poisson–Delaunay tessellation* (PDT). In Figure 1.3(b) a realization of a PDT is shown.

**Theorem 5.** *Let  $T$  be a PDT induced by a Poisson process with intensity  $\lambda$ . Then*

$$\lambda^{(0)} = \lambda, \quad \lambda^{(1)} = 3\lambda, \quad \lambda^{(2)} = 2\lambda, \quad \gamma = \frac{32}{3\pi} \sqrt{\lambda}.$$

*Proof.* Since  $\lambda^{(0)} = \lambda$  and  $\text{Ev}_0(\Xi^*) = 3$  we get with Theorem 3 that  $\lambda^{(1)} = 3\lambda, \lambda^{(2)} = 2\lambda$ . For the proof of  $\gamma = \frac{32}{3\pi} \sqrt{\lambda}$  see e.g. [16], Chapter 10.  $\square$

If  $T = \{\Xi_n\}$  is a PDT induced by the stationary Poisson process  $X$ , then the vertices of  $T$  are given by the points of  $X$ . Moreover, due to Slivnyak’s theorem, the random Delaunay tessellation  $T^*$  with respect to the Palm version  $X^*$  of  $X$  is given by the dual Delaunay tessellations corresponding to the Voronoi tessellations induced by  $X^* = X \cup \{o\}$ . Thus, the union of edges of  $T^*$  emanating from  $o$  can be regarded as the typical edge star  $E^*$  of  $T$ .

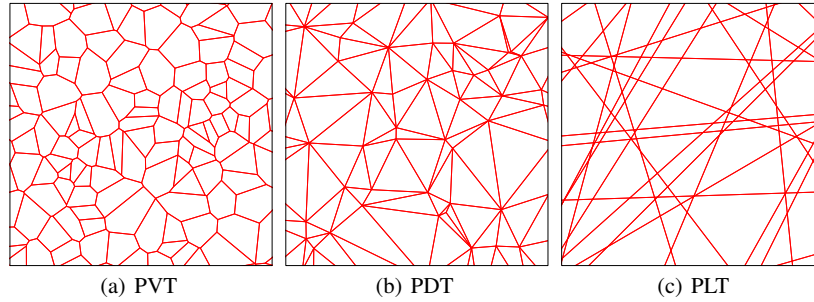


**Fig. 1.3** Realizations of tessellation models of Poisson type

### 1.1.4.3 Poisson line tessellation

Consider a stationary Poisson process  $\{R_n\}$  on the real line  $\mathbb{R}$  with (linear) intensity  $\tilde{\gamma} > 0$ . Each point  $R_n$  is independently marked with a random angle  $\Phi_n \sim U[0, \pi)$ . Then we can identify each pair  $(R_i, \Phi_i)$  with the line  $\ell_{(R_n, \Phi_n)} = \{(x, y) \in \mathbb{R}^2 : x \cos \Phi_n + y \sin \Phi_n = R_n\}$ . The resulting stationary random closed set  $\bigcup_{n \geq 1} \ell_{(R_n, \Phi_n)}$  is called a *Poisson line process* with intensity  $\tilde{\gamma}$ . It can be regarded as the edge set  $T^{(1)} = \bigcup_{n \geq 1} \ell_{(R_n, \Phi_n)}$  of a stationary tessellation  $T$  which is called a *Poisson line tessellation* (PLT). A realization of a PLT is displayed in Figure 1.3(c).

**Theorem 6.** *Let  $T$  be a PLT induced by a Poisson line process with intensity  $\tilde{\gamma}$ . Then*

$$\gamma = \tilde{\gamma}, \quad \lambda^{(0)} = \frac{1}{\pi} \tilde{\gamma}^2, \quad \lambda^{(1)} = \frac{2}{\pi} \tilde{\gamma}^2, \quad \lambda^{(2)} = \frac{1}{\pi} \tilde{\gamma}^2.$$

*Proof.* Note that  $\gamma = \mathbf{E}v_1(B_1(o) \cap \bigcup_{n \geq 1} \ell_{(R_n, \Phi_n)}) / \pi$  does not depend on the distribution of  $\Phi_1, \Phi_2, \dots$ , where  $B_r(x) = \{y \in \mathbb{R}^2 : |x - y| \leq r\}$  denotes the ball with midpoint  $x \in \mathbb{R}^2$  and radius  $r > 0$ . Thus,

$$\gamma = \mathbf{E}v_1(B_1(o) \cap \bigcup_{n \geq 1} \ell_{(R_n, 0)}) / \pi = \mathbf{E}v_1([0, 1]^2 \cap \bigcup_{n \geq 1} \ell_{(R_n, 0)}) = \tilde{\gamma}.$$

Theorem 3 with  $\mathbf{E}v_0(E^*) = 4$  yields  $\lambda^{(0)} = \lambda^{(2)}$  and  $\lambda^{(1)} = 2\lambda^{(0)}$ . Furthermore, it holds that  $\mathbf{E}v_1(S^*) = \gamma / \lambda^{(1)} = \pi / (2\gamma)$ , see e.g. [17]. Thus  $\lambda^{(1)} = \frac{2}{\pi} \gamma^2$ .  $\square$

## 1.2 Cox processes

In this section we introduce the notions of Cox processes and random measures associated with this class of point processes. Particular emphasis is put on the case that the driving measure of a Cox process  $\{X_n\}$  is concentrated on the edge set  $T^{(1)}$  of a stationary tessellation  $T$ , i.e., we assume that  $\mathbb{P}(X_n \in T^{(1)}) = 1$  for all  $n \in \mathbb{N}$ .

### 1.2.1 Cox processes and random measures

Cox processes can be regarded as generalizations of Poisson processes, containing them as a special case. The difference is that we now consider a random measure instead of the deterministic intensity measure  $\mu$  of Poisson processes. Thus, in order to define Cox processes we first have to introduce the notion of (locally finite) random measures, which can be seen as a generalization of random counting measures.

Let  $\mathbf{M} = \mathbf{M}(\mathbb{R}^2)$  denote the set of all locally finite measures on  $\mathcal{B}(\mathbb{R}^2)$ . On  $\mathbf{M}$  we define the  $\sigma$ -algebra  $\mathcal{M} = \mathcal{M}(\mathbb{R}^2)$  as the smallest  $\sigma$ -algebra such that the mappings  $\eta \mapsto \eta(B)$  are  $(\mathcal{M}, \mathcal{B}(\mathbb{R}^2))$ -measurable for all  $B \in \mathcal{B}_0(\mathbb{R}^2)$ . Thus, we obtain the measurable space  $(\mathbf{M}, \mathcal{M})$ . The shift operator  $t_x : \mathbf{M} \rightarrow \mathbf{M}$  on  $\mathbf{M}$  is defined in the same way as for counting measures, i.e.  $t_x \eta(B) = \eta(B + x)$  for all  $B \in \mathcal{B}(\mathbb{R}^2)$  and  $x \in \mathbb{R}^2$ , and we define the rotation operator  $\vartheta_R : \mathbf{M} \rightarrow \mathbf{M}$  by  $\vartheta_R \eta(B) = \eta(\vartheta_R^{-1} B) = \eta(\vartheta_{R^{-1}} B)$  for all rotations  $R : \mathbb{R}^2 \rightarrow \mathbb{R}^2$  around the origin.

A measurable mapping  $\Lambda : \Omega \rightarrow \mathbf{M}$  from some probability space  $(\Omega, \mathcal{A}, \mathbb{P})$  into the measurable space  $(\mathbf{M}, \mathcal{M})$  is then called *random measure* on  $\mathcal{B}(\mathbb{R}^2)$ . The random measure  $\Lambda$  is called *stationary* if  $t_x \Lambda \stackrel{d}{=} \Lambda$  for all  $x \in \mathbb{R}^2$ . In this case  $\mathbf{E}\Lambda(B) = \lambda v_2(B)$  for  $B \in \mathcal{B}(\mathbb{R}^2)$ , where  $\lambda \geq 0$  is some constant which is called the intensity of  $\Lambda$ . Notice that  $\lambda = \mathbf{E}\Lambda([0, 1]^2)$ . If  $0 < \lambda < \infty$ , we define the *Palm distribution* of  $\Lambda$  as the probability measure  $P_\Lambda^* : \mathcal{M} \rightarrow [0, 1]$  given by

$$P_\Lambda^*(A) = \frac{1}{\lambda} \mathbb{E} \left( \int_{[0, 1]^2} \mathbf{1}_A(t_x \Lambda) \Lambda(dx) \right), \quad A \in \mathcal{M}. \quad (1.9)$$

Assume now that a random measure  $\Lambda$  is given. The point process  $X$  is called a *Cox process* with random *driving measure*  $\Lambda$  if

$$\mathbb{P}(X(B_1) = k_1, \dots, X(B_n) = k_n) = \mathbf{E} \left( \prod_{i=1}^n \frac{\Lambda(B_i)^{k_i} e^{-\Lambda(B_i)}}{k_i!} \right) \quad (1.10)$$

for any  $k_1, \dots, k_n \in \mathbb{N}_0$  and pairwise disjoint  $B_1, \dots, B_n \in \mathcal{B}_0(\mathbb{R}^2)$ . Thus, given that  $\Lambda = \eta$  for some  $\eta \in \mathcal{M}$ , a Cox process  $X$  can be seen as a (conditional) Poisson process with intensity measure  $\eta$ , i.e., the distribution of a Cox process is a mixture of the distributions of (not necessarily stationary) Poisson processes. This is the reason why a Cox process is sometimes called a *doubly stochastic Poisson process*.

Note that the definition of Cox processes directly leads to a simulation method based on a two step procedure. First, a realization  $\eta$  of  $\Lambda$  is generated. Then, in the second step, a Poisson process with intensity measure  $\eta$  is simulated.

Now we summarize some basic properties of Cox processes. The following result is an immediate consequence of (1.10).

**Theorem 7.** *Let  $X$  be a Cox process with random driving measure  $\Lambda$ . Then  $X$  is stationary (resp. isotropic) if and only if  $\Lambda$  is stationary (resp. isotropic). If  $X$  is stationary, then its intensity is equal to the intensity  $\lambda$  of  $\Lambda$ .*

Classical examples of Cox processes are the Neyman-Scott process and the modulated Poisson process ([4]), see also HEINRICH (?) for further examples.

Recall that the Palm version  $X^* = X \cup \{o\}$  of a stationary Poisson process  $X$  is obtained by adding the origin  $o$  to  $X$ . This property of Poisson processes can be generalized to get the following result, which is called *Slivnyak's theorem* for Cox processes. Namely, the Palm distribution  $P_X^*$  of a stationary Cox process  $X$  with random driving measure  $\Lambda$  can be characterized as follows, see e.g. [17], p. 156.

**Theorem 8.** *Let  $X$  be a Cox process with stationary driving measure  $\Lambda$ . Then  $P_X^*(A) = \mathbb{P}(\tilde{X} \cup \{o\} \in A)$  for all  $A \in \mathcal{N}$ , where  $\tilde{X}$  is a Cox process with random driving measure  $\Lambda^*$  distributed according to the Palm distribution  $P_\Lambda^*$  of  $\Lambda$ .*

Thus, to simulate the Palm version  $X^*$  of a stationary Cox process  $X$ , we can use a two-step procedure. First, we generate a realization  $\eta^*$  of  $\Lambda^*$ . Afterwards, adding a point at the origin  $o$ , we simulate a Poisson process with intensity measure  $\eta^*$ .

## 1.2.2 Cox processes on the edges of random tessellations

In this section, we introduce a class of Cox processes  $X$  whose random driving measures are concentrated on the edge sets of random tessellations. Let  $T$  be a stationary random tessellation with length intensity  $\gamma = \mathbb{E}v_1([0, 1]^2 \cap T^{(1)})$  and, for some  $\lambda_\ell > 0$ , define the random measure  $\Lambda : \mathcal{B}(\mathbb{R}^2) \rightarrow [0, \infty]$  by

$$\Lambda(B) = \lambda_\ell v_1(B \cap T^{(1)}), \quad B \in \mathcal{B}(\mathbb{R}^2). \quad (1.11)$$

Notice that  $\Lambda$  is stationary. Its intensity is given by

$$\lambda = \lambda_\ell \mathbf{E} \nu_1([0, 1]^2 \cap T^{(1)}) = \lambda_\ell \gamma. \quad (1.12)$$

Let  $X$  be a Cox process whose random driving measure  $\Lambda$  is given by (1.11). Then, a direct application of Theorem 7 yields that  $X$  is stationary with intensity  $\lambda$  given in (1.12). Furthermore,  $X$  is isotropic if  $T$  is isotropic. Realizations of  $X$  can be generated by simulating first  $T$  and then simulating Poisson processes with (linear) intensity  $\lambda_\ell$  on each segment of  $T^{(1)}$ . In Figure 1.4 realizations of Cox processes on  $T^{(1)}$  are shown for  $T$  being a PDT and PVT, respectively.

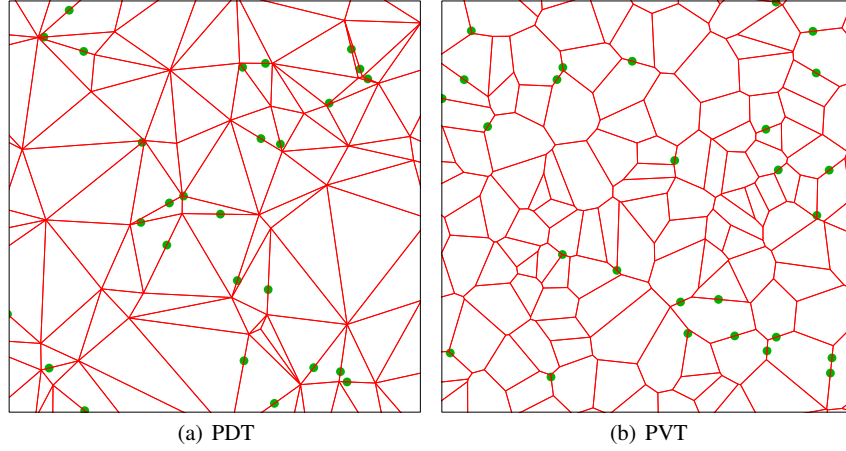


**Fig. 1.4** Realizations of Cox processes on PDT and PVT.

Recall that in Theorem 8 the Palm distribution of stationary Cox processes is characterized, which is uniquely determined by the Palm version  $\Lambda^*$  of the stationary driving measure  $\Lambda$ . For Cox processes on the edge set of stationary tessellations, the result of Theorem 8 can be specified in the following way.

**Theorem 9.** *Let  $\Lambda$  be the stationary random measure given in (1.11). Then  $\Lambda^*(B) = \lambda_\ell \nu_1(B \cap \tilde{T}^{(1)})$  for each  $B \in \mathcal{B}(\mathbb{R}^2)$ , where the tessellation  $\tilde{T}$  is distributed according to the Palm distribution  $P_{T^{(1)}}^*$  with respect to the 1-dimensional Hausdorff measure on  $T^{(1)}$ .*

*Proof.* Let  $\tau \in \mathbb{T}$  be an arbitrary tessellation. Then we can identify the measure  $\eta$  given by  $\eta(\cdot) = \lambda_\ell \nu_1(\cdot \cap \tau^{(1)})$  with  $\tau$ , writing  $\eta_\tau$ . It is easy to see that  $\eta_{t_x \tau} = t_x \eta_\tau$  for all  $x \in \mathbb{R}^2$ . Furthermore, using the definition of the Palm distribution  $P_\Lambda^*$  of  $\Lambda$  given in (1.9), we get for each  $A \in \mathcal{M}$  that  $P_\Lambda^*(A) = \lambda^{-1} \int_{\mathbb{M}} \int_{[0,1]^2} \mathbf{1}_A(t_x \eta) \eta(dx) P_\Lambda(d\eta)$ , i.e.

$$P_\Lambda^*(A) = \frac{1}{\gamma} \int_{\mathbb{T}} \int_{[0,1]^2 \cap \tau^{(1)}} \mathbf{1}_A(t_x \eta_\tau) \nu_1(dx) P_T(d\tau) = P_{T^{(1)}}^*(\{\tau \in \mathbb{T} : \eta_\tau \in A\}),$$

where the latter equality immediately follows from the definition of the Palm distribution  $P_{T^{(1)}}^*$  since  $\gamma = \mathbf{E}v_1(T^{(1)} \cap [0, 1]^2)$ . This means that the distributions of  $\Lambda^*$  and  $\eta_{\tilde{T}}(\cdot) = \lambda_\ell v_1(\cdot \cap \tilde{T}^{(1)})$  are equal.  $\square$

Note that  $\tilde{T}$  can be viewed as the random tessellation  $T$  under the condition that  $o \in T^{(1)}$ . Thus, under  $P_{T^{(1)}}^*$ , there is an edge  $\tilde{S}$  of  $\tilde{T}$  through  $o$  with probability 1. However, the distributions of  $\tilde{S}$  and the typical edge  $S^*$  do not coincide. This can be seen as follows. Assume that  $h : \mathcal{L}^o \rightarrow [0, \infty)$  is a translation-invariant measurable function and let  $S(x)$  denote the segment of  $T^{(1)}$  through  $x$  for  $x \in T^{(1)}$ . Then,

$$\begin{aligned} \mathbf{E}h(\tilde{S}) &= \frac{1}{\gamma} \mathbf{E} \int_{T^{(1)} \cap [0, 1]^2} h(S(x) - x) v_1(dx) \\ &= \frac{1}{\gamma} \mathbf{E} \sum_{(Y_i, S_i^o) \in T} h(S_i^o) \int_{S_i} \mathbf{1}_{[0, 1]^2}(x) v_1(dx) \\ &= \frac{\lambda^{(1)}}{\gamma} \mathbf{E}h(S^*) \int_{\mathbb{R}^2} \int_{S^*} \mathbf{1}_{[0, 1]^2 - y}(x) v_1(dx) v_2(dy) = \frac{1}{\mathbf{E}v_1(S^*)} \mathbf{E}v_1(S^*) h(S^*), \end{aligned}$$

where we used the refined Campbell theorem for stationary marked point processes (Theorem 1) and the mean-value formulae given in Theorem 3. Thus, the distribution of  $\tilde{S}$  can be represented as a length-weighted distribution of  $S^*$ .

For Cox processes on the edges of random tessellations the following scaling invariance can be observed. Let  $T$  be a stationary random tessellation with length intensity 1. Then we define the scaled tessellation  $T_\gamma$  as the random tessellation whose edge set is given by  $T_\gamma^{(1)} = \frac{1}{\gamma} T^{(1)}$ . Thus, the length intensity of  $T_\gamma$  is  $\gamma$  since  $\mathbf{E}v_1(T_\gamma^{(1)} \cap [0, 1]^2) = \mathbf{E}v_1(T^{(1)} \cap [0, \gamma]^2)/\gamma = \gamma$  due to the homogeneity of the Hausdorff measure  $v_1$ , see also KIDERLEN, Section 2.1.1.

Now let  $X = \{X_n\}$  be a Cox process on  $T_\gamma$  with linear intensity  $\lambda_\ell$  and let  $X' = \{X'_n\}$  be a Cox process on  $T_{\gamma'}$  whose linear intensity is given by  $\lambda'_\ell$ . Moreover, assume that the intensity quotients  $\kappa = \gamma/\lambda_\ell$  and  $\kappa' = \gamma'/\lambda'_\ell$  are equal, i.e.,  $\kappa = \kappa'$ . Then we get for any  $C \in \mathcal{C}$  that

$$\begin{aligned} \mathbb{P}(X(C) = 0) &= \mathbf{E} \exp(\lambda_\ell v_1(C \cap T_\gamma^{(1)})) \\ &= \mathbf{E} \exp\left(\frac{\lambda_\ell \gamma'}{\gamma} v_1\left(\frac{\gamma}{\gamma'} C \cap T_\gamma^{(1)}\right)\right) \\ &= \mathbb{P}\left(X'\left(\frac{\gamma}{\gamma'} C\right) = 0\right) = \mathbb{P}\left(\left(\frac{\gamma'}{\gamma} X'\right)(C) = 0\right), \end{aligned}$$

where the scaled point process  $\frac{\gamma'}{\gamma} X'$  is defined by  $\frac{\gamma'}{\gamma} X' = \{\frac{\gamma'}{\gamma} X'_n\}$ . Since the distribution of a point process  $X$  is uniquely determined by its void probabilities  $\mathbb{P}(X(C) = 0), C \in \mathcal{C}$ , we have that  $X \stackrel{d}{=} \frac{\gamma'}{\gamma} X'$ . Thus, for a given tessellation type  $T$ , the intensity quotient  $\kappa$  defines the Cox process  $X$  on the scaled tessellation  $T_\gamma$  with linear intensity  $\lambda_\ell$  uniquely up to a certain scaling. We therefore call  $\kappa$  the *scaling factor* of  $X$ . For numerical results it is therefore sufficient to focus on single

parameter pairs  $\gamma$  and  $\lambda_\ell$  for each value of  $\kappa$ . For other parameters with the same scaling factor  $\kappa$  the corresponding results can then be obtained by a suitable scaling.

### 1.3 Cox-Voronoi tessellations

In this section we consider Voronoi tessellations induced by stationary Coxian point processes. The typical cell of these so-called *Cox-Voronoi tessellations* can describe e.g. the typical serving zone of telecommunication networks. Unfortunately, its distribution is not known analytically. Even for the typical cell of PVT it is hard to obtain closed analytical expressions for the distribution of cell characteristics like the perimeter, the number of vertices, or the area. On the other hand, it is often possible to develop simulation algorithms for the typical Voronoi cell, which can be used to determine the distribution of cell characteristics approximatively. We discuss such simulation algorithms for two examples of Voronoi tessellations. To begin with, in Section 1.3.1, we first consider the case of the typical Poisson-Voronoi cell. Then, in Section 1.3.2, we show how the typical cell of a Cox-Voronoi tessellation  $T_X$  can be simulated if the random driving measure of the underlying Cox process  $X$  is concentrated on the edge set of a certain stationary tessellation  $T$ , where we assume that  $T$  is a PLT, see Figure 1.6(a).

In the ergodic case, the distribution of the typical cell can be obtained as the limit of empirical distributions of cells observed in a sequence of unboundedly increasing sampling windows, see Theorem 2. Thus, in order to approximate the distribution of the typical cell, we can simulate the random tessellation in a large sampling window  $W$ , considering spatial averages of those cells whose associated points belong to  $W$ . Alternatively, we can approximate this distribution by simulating independent copies of the typical cell and by taking sample means instead of spatial averages.

Note that there are several advantages of the latter approach. If we simulate the tessellation in a large sampling window, then the cells are correlated and there are edge effects which may be significant if  $W$  is not large enough. On the other hand, for large  $W$ , runtime and memory problems occur. However, these problems can be avoided if independent copies of the typical cell are simulated locally, but the challenge is then to develop such simulation algorithms. Recall that the typical Voronoi cell  $\Xi_X^*$  of any stationary point process  $X$  can be (locally) represented as  $\Xi_X^* = \bigcap_{n \in \mathbb{N}} H(o, X_n^*)$ , where  $X^* = \{X_n^*\}$  is the Palm version of  $X$ . Thus, suitable simulation algorithms for the points of  $X^*$  have to be developed.

#### 1.3.1 The Poisson case

We first show how stationary Poisson processes in  $\mathbb{R}^2$  can be simulated radially. Then, we use this result in order to develop a local simulation algorithm for the typical cell of PVT.

### 1.3.1.1 Simulation of stationary Poisson processes

In many applications it is useful to simulate the points of stationary Poisson processes in  $\mathbb{R}^2$  radially, i.e. with increasing distance to the origin. For this purpose, we first consider a stationary Poisson process  $Z = \{Z_n\}$  on the nonnegative half-line  $[0, \infty)$  denoting its (linear) intensity by  $\lambda > 0$ . Then, the points  $Z_n$  of  $Z$  can be given by  $Z_n = \lambda^{-1} \sum_{i=1}^n Y_i$  for each  $n \geq 1$ , where  $Y_1, Y_2, \dots$  is a sequence of independent and exponentially distributed random variables with  $Y_i \sim \text{Exp}(1)$  for each  $i \geq 1$ . This representation of  $Z$  can be used in order to radially simulate a stationary Poisson process in  $\mathbb{R}^2$  with the (planar) intensity  $\lambda$ .

Note that each point  $x = (x_1, x_2) \in \mathbb{R}^2$  can be represented by its polar coordinates, i.e.  $x = (r \cos \varphi, r \sin \varphi)$  with  $r \in [0, \infty)$  and  $\varphi \in [0, 2\pi)$ . Furthermore, consider a sequence  $\Phi_1, \Phi_2, \dots$  of independent and uniformly distributed random variables with  $\Phi_i \sim U[0, 2\pi)$  for each  $i \geq 1$ , assuming that  $\{\Phi_i\}$  and  $\{Y_i\}$  are independent. For each  $n \geq 1$ , put

$$X_n = (R_n \cos \Phi_n, R_n \sin \Phi_n), \quad \text{where } R_n = \sqrt{\sum_{i=1}^n Y_i / (\pi \lambda)}. \quad (1.13)$$

Then, the following result is true, see e.g. [15].

**Theorem 10.** *The point process  $X = \{X_n\}$  given by (1.13) is a stationary Poisson process in  $\mathbb{R}^2$  with intensity  $\lambda$ .*

Thus, based on the statement of Theorem 10, stationary Poisson processes in  $\mathbb{R}^2$  can be radially simulated just by simulating  $U[0, 2\pi)$ - and  $\text{Exp}(1)$ -distributed random variables, respectively. Note that Theorem 10 can easily be generalized to Poisson processes in  $\mathbb{R}^d$  for any  $d \geq 1$ .

Besides radial simulation, there are further algorithms to simulate stationary Poisson processes in a sampling window  $W \in \mathcal{B}_0(\mathbb{R}^2)$  such that  $0 < v_2(W) < \infty$ . For instance, we can simulate a stationary Poisson process  $X$  with intensity  $\lambda$  in  $W$  by first simulating the random variable  $X(W) \sim \text{Poi}(\lambda v_2(W))$  and then, given  $X(W) = n$ , by simulating the  $n$  points  $X_1, \dots, X_n$  of  $X$  in the window  $W$  as independent and uniformly distributed random variables in  $W$ . Although this procedure, based on so-called *complete spatial randomness* of stationary Poisson processes, seems to be easy, it is not suitable in order to simulate the typical cell of PVT. On the one hand, it is not known in advance how large the sampling window  $W$  has to be chosen in order to construct the typical cell. On the other hand, this procedure is computationally inefficient since often too many points are simulated in advance.

### 1.3.1.2 Local simulation of the typical Poisson-Voronoi cell

Recall that due to Slivnyak's theorem, the typical cell of a PVT can be regarded as the Voronoi cell at the origin with respect to  $X^* = X \cup \{o\}$ , where  $X = \{X_n\}$  is the underlying stationary Poisson process. Thus, we can place a point at  $o$ , simulate further points  $X_n$  of  $X$  radially and then construct the typical cell  $\Xi_X^* = \bigcap_{n \in \mathbb{N}} H(o, X_n)$  as intersection of the bisectors  $H(o, X_n)$  for  $n \geq 1$ .

More precisely, we simulate the points  $X_1, X_2, \dots$  successively, with increasing distance to the origin, until a bounded Voronoi cell at  $o$  can be constructed by the simulated points. We call this cell the *initial cell*. Afterwards, we check for each newly simulated point if the initial cell is influenced by points with larger distances from  $o$  than the latest generated point. If this is not the case, we stop the algorithm. Otherwise we simulate a further point. This local *simulation algorithm* of the typical Poisson-Voronoi cell is summarized below, where the points  $X_1, X_2, \dots$  are sampled using the random variables  $\Phi_1, \Phi_2, \dots, Y_1, Y_2, \dots$ , and  $R_1, R_2, \dots$  introduced in Section 1.3.1.1. The main steps of the algorithm are visualized in Figure 1.5.

1. Put  $X^* = \{o\}$ .
2. Simulate independent random variables  $\Phi_1, \Phi_2, \dots$  and  $Y_1, Y_2, \dots$  such that  $U_i \sim U[0, 2\pi)$  and  $Y_i \sim \text{Exp}(1)$  for  $i = 1, 2, \dots$ .
3. Compute the points  $X_1, \dots, X_n$  by (1.13) and add them to  $X^*$  until an (compact) initial cell  $\Xi_X^*$  at  $o$  can be constructed from  $X^*$ .
4. If  $R_n \geq r_{max} = 2 \max\{|v_i|\}$ , were  $\{v_i\}$  is the set of vertices of  $\Xi_X^*$ , then stop, else add further points to  $X^*$  and update  $\Xi_X^*$ .

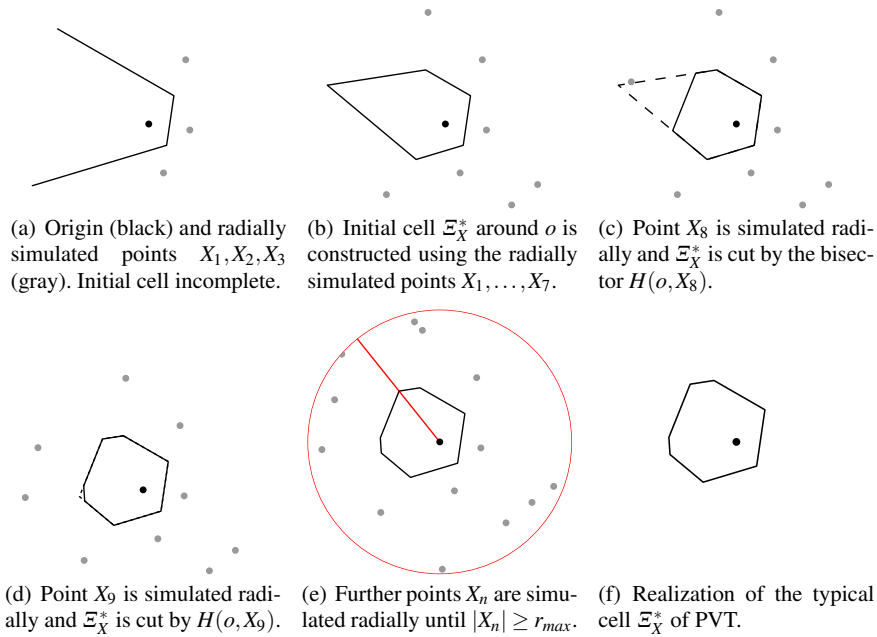


**Fig. 1.5** Simulation of the typical cell of PVT

When implementing this simulation algorithm we have to take into account some technical details. First, a rule for constructing the initial cell has to be implemented. If for some  $n \geq 3$  the points  $X_1, \dots, X_n$  have been generated, then we can use a cone criterion in order to check if a bounded Voronoi cell can be constructed around  $o$  by

these points. Once the initial cell  $\Xi_X^*$  has been generated, points of  $X^*$  outside the ball  $B_{r_{\max}}(o)$  cannot influence the typical cell anymore since the bisector between  $o$  and any  $x \in B_{r_{\max}}(o)^c$  does not intersect  $\Xi_X^*$ . Thus, the simulation stops if  $R_n \geq r_{\max}$ .

### 1.3.2 Cox processes on the edges of PLT

We now consider Cox processes  $X = \{X_n\}$  whose random driving measure  $\Lambda$  is concentrated on the edges of a stationary random tessellation  $T$ , where we assume that  $\Lambda$  is given by (1.11). In particular, the typical cell  $\Xi_X^*$  of the Voronoi tessellation  $T_X = \{\Xi_{X,n}\}$  induced by  $X$  will be investigated. Recall that  $T_X$  can be identified with the marked point process  $\{(X_n, \Xi_{X,n}^o)\}$ , where  $\Xi_{X,n}^o = \Xi_{X,n} - X_n$  denotes the centered version of the Voronoi cell  $\Xi_{X,n}$  at  $X_n$  with respect to  $X$ , see Figure 1.6.

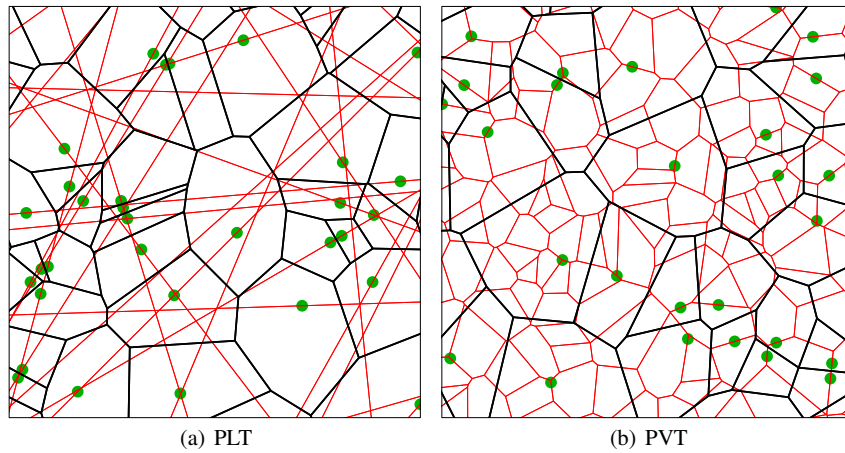


**Fig. 1.6** Realizations of  $T_X$  for Cox processes on PLT and PVT.

If the Cox process  $X$  models the locations of network components in telecommunication networks, then  $\Xi_{X,n}$  can be regarded as the area of influence of the network component at  $X_n$ , where  $\Xi_{X,n}$  is called the *serving zone* of  $X_n$ . Thus, the typical cell  $\Xi_X^*$  of  $T_X$  is an important characteristic in global econometric analysis and planning of telecommunication networks, because various cost functionals of hierarchical network models can be represented as expectations of functionals of  $\Xi_X^*$ , see also Section 1.4.

As we already mentioned at the beginning of Section 1.3, suitable simulation algorithms for the points of the Palm version  $X^*$  of  $X$  have to be developed in order to locally simulate the typical cell  $\Xi_X^*$  of the Cox-Voronoi tessellation  $T_X$ . However, in contrast to the situation discussed in Section 1.3.1.2, we do not simulate the points of  $X^*$  radially, at least not at once, when considering Cox processes on PDT, PLT

and PVT, respectively. But we simulate the points of the Poisson process radially which induces the Palm version of the underlying tessellation (regarded as random Hausdorff measure), alternatingly with the points of the (linear) Poisson processes on the edges of this tessellation. As an example, we show how this can be done for Cox processes on PLT.

### 1.3.2.1 Palm version of PLT

Let  $X$  be a stationary Cox process with linear intensity  $\lambda_\ell$  on a stationary PLT  $T$  with length intensity  $\gamma$ . Note that due to Theorems 8 and 9 it holds that  $X^* = \tilde{X} \cup \{o\}$ , where  $\tilde{X}$  is a Cox process on the Palm version  $\tilde{T}$  of  $T$  regarded as the random Hausdorff measure  $\nu_1(\cdot \cap T^{(1)})$  on  $T^{(1)}$ . Thus, in a first step,  $T$  has to be simulated according to its Palm distribution with respect to  $\nu_1(\cdot \cap T^{(1)})$ , i.e., under the condition that  $o \in T^{(1)}$ . It turns out that the edge set  $\tilde{T}^{(1)}$  of this conditional PLT can be constructed just by adding an isotropic line through  $o$  to  $T^{(1)}$ .

**Theorem 11.** *Let  $T^{(1)}$  be the edge set of a stationary PLT with intensity  $\gamma$  and let  $\ell(\Phi)$  be a line through the origin with random direction  $\Phi \sim \mathbf{U}[0, \pi)$  which is independent of  $T^{(1)}$ . Then  $\tilde{T}^{(1)} \stackrel{d}{=} T^{(1)} \cup \ell(\Phi)$ .*

*Proof.* Since the distribution of a random closed set is uniquely determined by its capacity functional (MOLCHANOV), we show that the capacity functionals of  $\tilde{T}^{(1)}$  and  $T^{(1)} \cup \ell(\Phi)$  coincide. With the notation  $T^{(1)} = \bigcup_{n \geq 1} \ell_{(R_n, \Phi_n)}$  introduced in Section 1.1.4.3, the definition of the Palm distribution of stationary random measures (see (1.9)) gives that for each  $C \in \mathcal{C}$

$$\mathbb{P}(\tilde{T}^{(1)} \cap C \neq \emptyset) = \frac{1}{\pi\gamma} \mathbf{E} \int_{T^{(1)} \cap B_1(o)} \mathbf{1}_{\{\bigcup_{n \geq 1} (\ell_{(R_n, \Phi_n)} - x) \cap C \neq \emptyset\}} \nu_1(dx).$$

Note that the number  $N$  of lines of a Poisson line process which intersect a convex compact set  $W \subset \mathbb{R}^2$  is  $\text{Poi}(\lambda)$ -distributed with  $\lambda = \gamma \nu_1(\partial W)/\pi$  and, given  $N = k$ , these  $k$  lines  $\ell_1, \dots, \ell_k$  are independent and isotropic uniform random (IUR), see KIDERLEN. Thus, for  $W = B_{R(C)+1}(o)$ , where  $R(C) = \sup_{x \in C} \{|x|\}$ , we get

$$\begin{aligned} \mathbb{P}(\tilde{T}^{(1)} \cap C \neq \emptyset) &= \sum_{k=0}^{\infty} \frac{\mathbb{P}(N=k)}{\pi\gamma} \sum_{i=1}^k \mathbf{E} \left( \int_{\ell_i \cap B_1(o)} \mathbf{1}_{\{\bigcup_{i=1}^k (\ell_i - x) \cap C \neq \emptyset\}} \nu_1(dx) \mid N=k \right) \\ &= \frac{1}{\pi\gamma} \sum_{k=0}^{\infty} \frac{e^{-\lambda} \lambda^k}{k!} k \mathbf{E} \left( \int_{\ell_1 \cap B_1(o)} \mathbf{1}_{\{\bigcup_{i=1}^k (\ell_i - x) \cap C \neq \emptyset\}} \nu_1(dx) \mid N=k \right) \\ &= \frac{\lambda}{\pi\gamma} \sum_{k=0}^{\infty} \frac{e^{-\lambda} \lambda^k}{k!} \mathbf{E} \left( \int_{\ell_1 \cap B_1(o)} \mathbf{1}_{\{\bigcup_{i=1}^{k+1} (\ell_i - x) \cap C \neq \emptyset\}} \nu_1(dx) \mid N=k+1 \right). \end{aligned}$$

Since the lines  $\ell_1, \ell_2, \dots, \ell_{k+1}$  are independent and IUR, we can consider  $\ell_1$  separately, where the remaining  $\ell_2, \dots, \ell_{k+1}$  still are independent of each other, IUR, and independent of  $\ell_1$ . This gives

$$\begin{aligned} \mathbb{P}(\tilde{T}^{(1)} \cap C \neq \emptyset) &= \frac{\lambda}{\pi\gamma} \mathbb{P}((T^{(1)} \cup \ell(\Phi)) \cap C \neq \emptyset) \mathbf{E}v_1(\ell_1 \cap B_1(o)) \\ &= \mathbb{P}((T^{(1)} \cup \ell(\Phi)) \cap C \neq \emptyset), \end{aligned}$$

where in the last equality we used that  $\mathbf{E}v_1(\ell_1 \cap B_1(o)) = \pi^2/v_1(\partial W)$ , see e.g. KIDERLEN, formula (2.5).  $\square$

### 1.3.2.2 Local simulation of the typical Cox-Voronoi cell

Using Theorem 11, we are able to briefly describe the main idea of an algorithm for local simulation of the typical cell  $\Xi_X^*$  of the Voronoi tessellation  $T_X = \{\Xi_{X,n}\}$  induced by the Cox process  $X$  on PLT.

We first put a line  $\ell(\Phi)$  with direction  $\Phi \sim U[0, \pi)$  through the origin  $o$  and then, on both half-lines of  $\ell(\Phi)$  seen from  $o$ , we simulate the nearest points to  $o$  of a Poisson process with intensity  $\lambda_\ell$ . Next, we simulate independent random variables  $\Phi_1$  and  $R_1 (= Y_1)$  with  $\Phi_1 \sim U[0, 2\pi)$  and  $R_1 \sim \text{Exp}(2\gamma)$  and construct the line  $\ell_{(R_1, \Phi_1)} = \{(x, y) \in \mathbb{R}^2 : x \cos \Phi_1 + y \sin \Phi_1 = R_1\}$ . Note that  $\ell_{(R_1, \Phi_1)}$  is the closest line to the origin of a Poisson line process with length intensity  $\gamma$ . Then, on  $\ell_{(R_1, \Phi_1)}$ , we simulate points of a Poisson process with intensity  $\lambda_\ell$ . In the next step, we simulate independent random variables  $\Phi_2$  and  $Y_2$  with  $\Phi_2 \sim U[0, 2\pi)$  and  $Y_2 \sim \text{Exp}(2\gamma)$  constructing the line  $\ell_{(R_2, \Phi_2)} = \{(x, y) \in \mathbb{R}^2 : x \cos \Phi_2 + y \sin \Phi_2 = R_2\}$ , where  $R_2 = R_1 + Y_2$ , and so on.

In this way, similar to the algorithm discussed in Section 1.3.1.2, we simulate points of  $X^*$  in a neighborhood of the origin until a bounded Voronoi cell at  $o$  can be constructed by the simulated points. Afterwards, we check for each newly simulated point if this initial cell is influenced by points with larger distances from  $o$  than the latest generated point. If this is not the case, we stop the algorithm. Otherwise we continue to alternatingly simulate lines and points on them respectively. For further technical details of the simulation algorithm we refer to [6].

Similar algorithms can be constructed for local simulation of the typical Voronoi cell of stationary Cox processes on PVT and PDT, respectively, see [5, 19].

## 1.4 Typical connection lengths in hierarchical network models

We now consider two Cox processes simultaneously. The leading measures of either one or both of these Cox processes are concentrated on the edge set of a stationary tessellation, where we assume that the Cox processes are jointly stationary. We discuss representation formulae which have been derived in [19] for the distribution function and density of the typical Euclidean (i.e. direct) connection length  $D^*$  between certain pairs of points, chosen at random, one from each of the Cox processes. Furthermore, the typical shortest path length  $C^*$  is considered which is needed to connect such pairs of points along the edges of the underlying tessellation. A useful

tool in investigating these characteristics is Neveu's exchange formula (see e.g. [14]) for jointly stationary marked point processes, which is stated in Section 1.4.1. Then, in Section 1.4.2, we give a motivation of our investigations, where we explain how the results can be applied e.g. in econometric analysis and planning of hierarchical telecommunication networks.

### 1.4.1 Neveu's exchange formula

Let  $X^{(1)} = \{(X_n^{(1)}, M_n^{(1)})\}$  and  $X^{(2)} = \{(X_n^{(2)}, M_n^{(2)})\}$  be jointly stationary marked point processes with mark spaces  $\mathbb{M}_1$  and  $\mathbb{M}_2$ , respectively, and let  $\mathbb{N}_{\mathbb{M}_1, \mathbb{M}_2} = \mathbb{N}_{\mathbb{M}_1} \times \mathbb{N}_{\mathbb{M}_2}$  denote the product space of the families of simple and locally finite counting measures with marks in  $\mathbb{M}_1$  and  $\mathbb{M}_2$ , respectively, equipped with product- $\sigma$ -algebra  $\mathcal{N}_{\mathbb{M}_1} \otimes \mathcal{N}_{\mathbb{M}_2}$ . We then put  $Y = (X^{(1)}, X^{(2)})$  which can be regarded as a random element of  $\mathbb{N}_{\mathbb{M}_1, \mathbb{M}_2}$ . Let  $\lambda_1$  and  $\lambda_2$  denote the intensities of  $X^{(1)}$  and  $X^{(2)}$ , respectively, and assume that the shift operator  $t_x$  is defined by  $t_x Y = (t_x X^{(1)}, t_x X^{(2)})$  for  $x \in \mathbb{R}^2$ . Thus,  $t_x$  shifts the points of both  $X^{(1)}$  and  $X^{(2)}$  by  $-x \in \mathbb{R}^2$ . Note that  $t_x Y \stackrel{d}{=} Y$  for each  $x \in \mathbb{R}^2$  since  $X^{(1)}$  and  $X^{(2)}$  are jointly stationary. The *Palm distributions*  $P_Y^{(i)}$ ,  $i = 1, 2$  on  $\mathcal{N}_{\mathbb{M}_1} \otimes \mathcal{N}_{\mathbb{M}_2} \otimes \mathcal{B}(\mathbb{M}_i)$  with respect to the  $i$ -th component of  $Y$  are probability measures defined by

$$P_Y^{(i)}(A \times G) = \frac{1}{\lambda_i} \mathbf{E} \#\{n : X_n^{(i)} \in [0, 1)^2, M_n^{(i)} \in G, t_{X_n^{(i)}} Y \in A\} \quad (1.14)$$

for  $A \in \mathcal{N}_{\mathbb{M}_1} \otimes \mathcal{N}_{\mathbb{M}_2}$  and  $G \in \mathcal{B}(\mathbb{M}_i)$ . In particular, for  $A \in \mathcal{N}_{\mathbb{M}_i}$ ,  $G \in \mathcal{B}(\mathbb{M}_i)$ , we get  $P_Y^{(1)}(A \times \mathbb{N}_{\mathbb{M}_2} \times G) = P_{X^{(1)}}^*(A \times G)$  if  $i = 1$ , and  $P_Y^{(2)}(\mathbb{N}_{\mathbb{M}_1} \times A \times G) = P_{X^{(2)}}^*(A \times G)$  if  $i = 2$ , where  $P_{X^{(1)}}^*$  and  $P_{X^{(2)}}^*$  are the ordinary Palm distributions of the marked point processes  $X^{(1)}$  and  $X^{(2)}$ , respectively, introduced in (1.2).

Note that we also use the notation  $P_{X^{(i)}}^*$  for the Palm distribution  $P_Y^{(i)}$  of the vector  $(X^{(1)}, X^{(2)})$  in order to emphasize the dependence on  $X^{(i)}$  for  $i = 1, 2$ . With the definitions and notation introduced above, and writing  $\psi = (\psi^{(1)}, \psi^{(2)})$  for the elements of  $\mathbb{N}_{\mathbb{M}_1, \mathbb{M}_2}$ , *Neveu's exchange formula* can be stated as follows, see e.g. [11].

**Theorem 12.** *For any measurable  $f : \mathbb{R}^2 \times \mathbb{M}_1 \times \mathbb{M}_2 \times \mathbb{N}_{\mathbb{M}_1, \mathbb{M}_2} \rightarrow [0, \infty)$ , it holds that*

$$\begin{aligned} & \lambda_1 \int_{\mathbb{N}_{\mathbb{M}_1, \mathbb{M}_2} \times \mathbb{M}_1} \int_{\mathbb{R}^2 \times \mathbb{M}_2} f(x, m_1, m_2, t_x \psi) \psi^{(2)}(d(x, m_2)) P_Y^{(1)}(d(\psi, m_1)) \\ &= \lambda_2 \int_{\mathbb{N}_{\mathbb{M}_1, \mathbb{M}_2} \times \mathbb{M}_2} \int_{\mathbb{R}^2 \times \mathbb{M}_1} f(-x, m_1, m_2, \psi) \psi^{(1)}(d(x, m_1)) P_Y^{(2)}(d(\psi, m_2)). \end{aligned}$$

Neveu's exchange formula given in Theorem 12 allows to express the (conditional) distribution of functionals of a vector  $(X^{(1)}, X^{(2)})$  of jointly stationary point processes, seen from the perspective of the Palm distribution  $P_{X^{(1)}}^*$ , by the distribu-

tion of the same functional under  $P_{X^{(2)}}^*$ . This means that we can switch from the joint distribution of  $(X^{(1)}, X^{(2)})$  conditioned on  $o \in \{X_n^{(1)}\}$  to the joint distribution of  $(X^{(1)}, X^{(2)})$  conditioned on  $o \in \{X_n^{(2)}\}$ .

### 1.4.2 Hierarchical network models

Models from stochastic geometry have been used since more than 10 years in order to describe and analyze telecommunication networks, see e.g. [1, 8, 22]. However, the infrastructure of the network, like road systems or railways, has been included into the model rather seldom.

In this section we introduce spatial stochastic models for telecommunication networks with two hierarchy levels which take the underlying infrastructure of the network into account. In particular, we model the network infrastructure, e.g. road systems or railways, by the edge set  $T^{(1)}$  of a stationary tessellation  $T$  with (length) intensity  $\gamma = \mathbf{E}v_1(T^{(1)} \cap [0, 1]^2) > 0$ . The locations of both high and low level components (HLC, LLC) of the network are modelled by stationary point processes  $H = \{H_n\}$  and  $L = \{L_n\}$ , respectively, where  $H$  is assumed to be a Cox process on  $T^{(1)}$  whose random driving measure is given by (1.11), with linear intensity  $\lambda_\ell > 0$  and (planar) intensity  $\lambda = \lambda_\ell \gamma$ . Regarding the point process  $L$  we distinguish between two different scenarios. On the one hand, we consider the case that  $L$  is a stationary (planar) Poisson process with intensity  $\lambda'$  which is independent of  $T$  and  $H$ . On the other hand, we assume that  $L$  is a Cox process whose random driving measure is concentrated on the same edge set  $T^{(1)}$  as  $H$  and given by (1.11), but now with linear intensity  $\lambda'_\ell$ . Furthermore, we assume that  $L$  is conditionally independent of  $H$  given  $T$ . Thus, in the latter case, the planar intensity  $\lambda'$  of  $L$  is given by  $\lambda' = \lambda'_\ell \gamma$ .

#### 1.4.2.1 Typical serving zone

Each LLC of the network is connected with one of the HLC, i.e., each point  $L_n$  of  $L$  is linked to some point  $H_n$  of  $H$ . In order to specify this connection rule, so-called serving zones are considered, which are domains associated to each HLC such that the serving zones of distinct HLC do not overlap, but their union covers the whole region considered. Then a LLC is linked to that HLC in whose serving zone it is located. In the following, we assume that the *serving zones* of HLC are given by the cells of the stationary Voronoi tessellation  $T_H = \{\mathcal{E}_{H,n}\}$  induced by  $H$ . Thus, the point  $L_n$  is linked to the point  $H_j$  iff  $L_n \in \mathcal{E}_{H,j}$ , i.e., all LLC inside  $\mathcal{E}_{H,j}$  are linked to  $H_j$ , see Figure 1.7. The typical cell  $\mathcal{E}_H^*$  of  $T_H$  is called the *typical serving zone*.

However, note that more complex models for (not necessarily convex) serving zones can be considered as well, like Laguerre tessellations ([10]) or aggregated Voronoi tessellations ([18]).

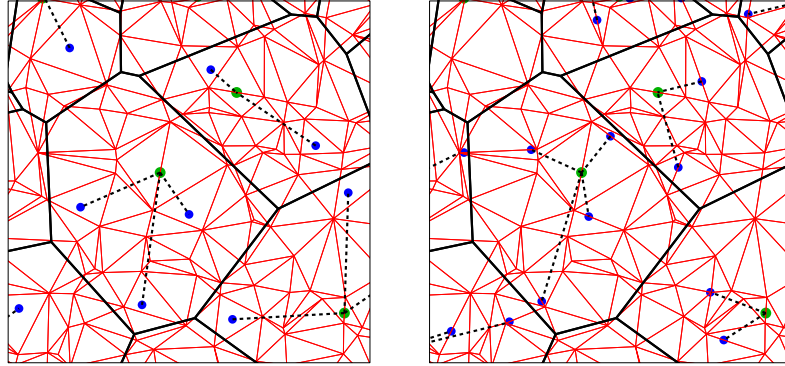


**Fig. 1.7** Cox process  $H$  on PDT with serving zones (black) and direct connection lengths (dashed) for  $L$  Poisson (left) and Cox (right)

Furthermore, we define the stationary marked point process  $H_S = \{(H_n, S_{H,n}^o)\}$ , where the marks are given by  $S_{H,n}^o = (T^{(1)} \cap \Xi_{H,n}) - H_n$ . Thus, each point  $H_n$  of  $H$  is marked with the segment system contained inside its serving zone. If  $L$  is a Cox process on  $T$ , then the point  $L_n$  of  $L$  is connected to  $H_j$  iff  $L_n \in S_{H,j}^o + H_j$ . It is easy to see that  $H_S$  is a stationary marked point process with intensity  $\lambda$  whose mark space is given by the family of finite segment systems  $\mathcal{L}^o$  which contain the origin. In particular, the typical mark  $S_H^* : \Omega \rightarrow \mathcal{L}^o$  of  $H_S$  is a random segment system which contains the origin, where  $S_H^*$  is called the *typical segment system* within the typical serving zone  $\Xi_H^*$ , see also Section 1.3.2.

#### 1.4.2.2 Typical connection lengths

So far, we introduced the four modelling components  $T$ ,  $L$ ,  $H_S$  and  $T_H$ . They can be used in order to define the stationary marked point process  $L_D = \{(L_n, D_n)\}$ , where  $D_n = |L_n - H_j|$  is the Euclidean distance between  $L_n$  and  $H_j$  provided that  $L_n \in \Xi_{H,j}$ . We are then interested in the distribution of the typical mark  $D^*$  of  $L_D$  which we call the *typical direct connection length* or, briefly, the *typical Euclidean distance*.

Realizations of the distances  $D_n$  for two different models of  $L$  are displayed in Figure 1.7, where the underlying tessellation  $T$  is a PDT; see also Figure 1.8. Note that realizations of the marked point process  $L_D$  can be constructed from realizations of  $L$  and  $H_S$  if  $L$  is a Cox process and from realizations of  $L$  and  $T_H$  if  $L$  is a Poisson process. Hence, instead of  $L_D$ , we can consider the vectors  $Y = (L, H_S)$  and  $Y = (L, T_H)$ , respectively, together with the Palm distribution  $P_L^*$  of  $Y$  with respect to the first component  $L$  introduced in (1.14).

Suppose now that  $(L^*, \tilde{H}_S)$  and  $(L^*, \tilde{T}_H)$ , respectively, are distributed according to the Palm distribution  $P_L^*$ , where we use the notation  $\tilde{H} = \{\tilde{H}_n\}$ ,  $\tilde{H}_S = \{(\tilde{H}_n, \tilde{S}_{H,n}^o)\}$

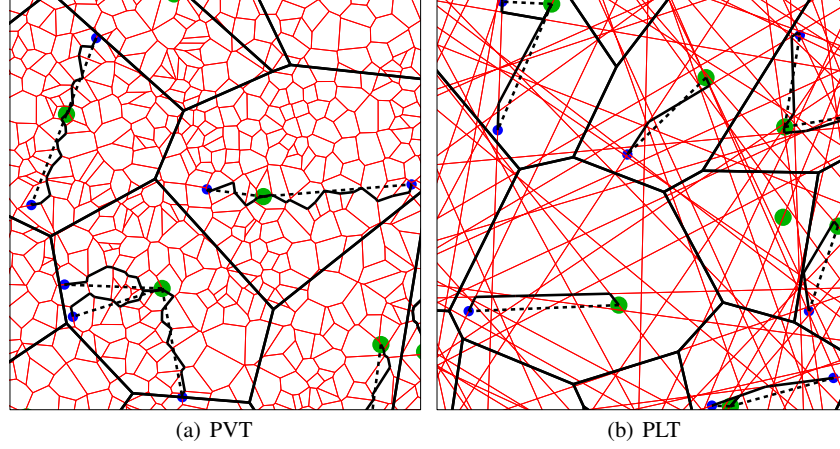


**Fig. 1.8** Euclidean distances and shortest paths along the edge system.

and  $\tilde{T}^{(1)} = \bigcup_{n \geq 1} (\tilde{S}_{H,n}^o + \tilde{H}_n)$ . Then  $D^*$  can be regarded as the distance from  $o$  to the point  $\tilde{H}_n$  of  $\tilde{H}$  in whose serving zone  $o$  is located. Note that  $L^* \setminus \{o\}$  is a stationary Poisson process resp. a Cox process on  $\tilde{T}$  if  $L$  is a Poisson process resp. a Cox process on  $T$ . In the same way we regard the vectors  $(\tilde{L}, H_S^*)$  and  $(\tilde{L}, T_H^*)$  which are distributed according to the Palm distributions  $P_{H_S^*}$  and  $P_{T_H^*}$ , respectively. Here we denote with  $T^{*(1)}$  the edge set of  $H_S^*$ . On the one hand, if  $L$  is a Cox process on  $T$ , then  $\tilde{L}$  is a (non-stationary) Cox process on  $T^{*(1)}$  with linear intensity  $\lambda'_\rho$ , which is conditionally independent of  $H^*$  given  $T^{*(1)}$ . On the other hand, if  $L$  is a stationary Poisson process which is independent of  $T$  and  $H$ , then  $\tilde{L} \stackrel{d}{=} L$ .

If  $L$  is a Cox process on  $T$ , then besides  $L_D = \{(L_n, D_n)\}$ , we consider the point process  $L_C = \{(L_n, C_n)\}$ , where  $C_n$  is the shortest path length from  $L_n$  to  $H_j$  along the edges of  $T$ , provided that  $L_n \in \Xi_{H,j}$ , see Figure 1.8. We are interested in the distribution of the *typical shortest path length*, i.e., the typical mark  $C^*$  of  $L_C$ .

### 1.4.3 Distributional properties of $D^*$ and $C^*$

We show that the distribution function and density of the typical (direct) connection length  $D^*$  can be expressed as expectations of functionals of the typical serving zone and its typical segment system. Furthermore, the density of the typical shortest path length  $C^*$  is considered.

Applying Neveu's exchange formula stated in Theorem 12 we can represent the distribution function of  $D^*$  in terms of the typical Voronoi cell  $\Xi_H^*$  of  $H$  if  $L$  is a planar Poisson process, and in terms of the typical segment system  $S_H^*$  if  $L$  is a Cox

process on  $T^{(1)}$ . This shows that the distribution of  $D^*$  is uniquely determined by  $T_H$  and  $H_S$ , respectively.

### 1.4.3.1 Distribution function of $D^*$

Note that the representation formulae stated in Theorem 13 below do not depend on  $L$  at all. The random closed sets  $\Xi_H^* \cap B_x(o)$  and  $S_H^* \cap B_x(o)$  occurring on the right-hand sides of (1.15) and (1.16) are illustrated in Figure 1.9.

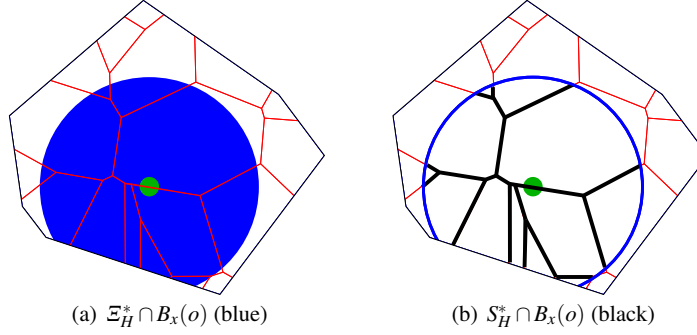


**Fig. 1.9** Typical serving zone and its typical segment system intersected by  $B_x(o)$ .

**Theorem 13.** (i) If  $L$  is a planar Poisson process that is independent of  $T$  and  $H$ , then the distribution function  $F_{D^*} : [0, \infty) \rightarrow [0, 1]$  of  $D^*$  is given by

$$F_{D^*}(x) = \lambda_\ell \gamma \mathbf{E} v_2(\Xi_H^* \cap B_x(o)), \quad x \geq 0, \quad (1.15)$$

where  $v_2(\Xi_H^* \cap B_x(o))$  denotes the area of  $\Xi_H^*$  intersected with the ball  $B_x(o) \subset \mathbb{R}^2$ . (ii) If  $L$  is a Cox processes on  $T^{(1)}$  which is conditionally independent of  $H$  given  $T$ , then the distribution function of  $D^*$  is given by

$$F_{D^*}(x) = \lambda_\ell \mathbf{E} v_1(S_H^* \cap B_x(o)), \quad x \geq 0. \quad (1.16)$$

*Proof.* Let us first assume that  $L$  is a planar Poisson process with intensity  $\lambda'$  and regard the vector  $Y = (L_D, T_H)$  as a random element of  $\mathbf{N}_{[0, \infty), \mathcal{P}^o}$ , where we use the notation  $(L_D^*, T_{\tilde{H}})$  and  $(\tilde{L}_D, T_H^*)$  introduced in Section 1.4.2.2 for the Palm versions of  $Y$  distributed according to  $P_{L_D}^*$  and  $P_{T_H}^*$ , respectively. For some measurable function  $h : [0, \infty) \rightarrow [0, \infty)$  we consider  $f : \mathbb{R}^2 \times [0, \infty) \times \mathcal{P}^o \times \mathbf{N}_{[0, \infty), \mathcal{P}^o} \rightarrow [0, \infty)$  defined by

$$f(x, m, \xi, \psi) = \begin{cases} h(m) & \text{if } o \in \xi + x, \\ 0 & \text{otherwise.} \end{cases}$$

Then, applying Theorem 12, we get

$$\begin{aligned}
\mathbb{E}h(D^*) &= \int_{\mathbb{N}_{[0,\infty)}, \mathcal{D}^o} \int_{\mathbb{R}^2 \times \mathcal{D}^o} f(x, \xi, m, \psi) \psi^{(2)}(d(x, \xi)) P_{L_D}^*(d(\psi, m)) \\
&= \frac{\lambda}{\lambda'} \int_{\mathbb{N}_{[0,\infty)}, \mathcal{D}^o} \int_{\mathbb{R}^2 \times [0,\infty)} f(-x, \xi, m, t_x \psi) \psi^{(1)}(d(x, m)) P_{T_H}^*(d(\psi, \xi)) \\
&= \frac{\lambda}{\lambda'} \int_{\mathbb{N}_{[0,\infty)}, \mathcal{D}^o} \int_{\mathbb{R}^2 \times [0,\infty)} h(|x|) \mathbf{1}_\xi(x) \psi^{(1)}(d(x, m)) P_{T_H}^*(d(\psi, \xi)) \\
&= \frac{\lambda}{\lambda'} \mathbf{E} \left( \mathbf{E} \left( \sum_{\tilde{L}_n \in \mathfrak{E}_H^*} h(|\tilde{L}_n|) \mid \mathfrak{E}_H^* \right) \right).
\end{aligned}$$

Since  $L$  and  $H$  are independent, we get that  $T_H^*$  and  $\tilde{L}$  are also independent and in addition that  $\tilde{L} \stackrel{d}{=} L$ . Thus, given  $\mathfrak{E}_H^*$ , we get that  $\tilde{L}$  is a stationary Poisson process of intensity  $\lambda'$ . Using Campbell's formula (see Theorem 1), we obtain

$$\mathbf{E} \left( \sum_{\tilde{L}_n \in \mathfrak{E}_H^*} h(|\tilde{L}_n|) \mid \mathfrak{E}_H^* \right) = \lambda' \int_{\mathfrak{E}_H^*} h(|u|) \nu_2(du)$$

which yields for  $h(|u|) = \mathbf{1}_{[0,x]}(|u|)$  that  $F_{D^*}(x) = \mathbf{E} \mathbf{1}_{[0,x]}(D^*) = \lambda \mathbf{E} \nu_2(\mathfrak{E}_H^* \cap B_x(o))$ . On the other hand, if  $L$  is a Cox process on  $T^{(1)}$ , then we regard the vector  $Y = (L_D, H_S)$  as a random element of  $\mathbb{N}_{[0,\infty), \mathcal{D}^o}$ . Recall that we use the notation  $(L_D^*, \tilde{H}_S)$  and  $(\tilde{L}_D, H_S^*)$  for the Palm versions of  $Y$  with respect to the Palm distributions  $P_{L_D}^*$  and  $P_{H_S^*}^*$ , respectively. Similar as above, an appropriate application of Neveu's exchange formula stated in Theorem 12 yields

$$\mathbb{E}h(D^*) = \frac{\lambda}{\lambda'} \mathbb{E} \left( \mathbb{E} \left( \sum_{\tilde{L}_n \in S_H^*} h(|\tilde{L}_n|) \mid S_H^* \right) \right).$$

Note that  $\tilde{L}$  is independent of  $H_S^*$  under  $P_{H_S^*}^*$  given  $S_H^*$ . Furthermore,  $\lambda' = \lambda'_\ell \gamma$  and  $\tilde{L} \cap S_H^*$  is a Cox process whose random intensity measure is given by  $\lambda'_\ell \nu_1(B \cap S_H^*)$  for  $B \in \mathcal{B}(\mathbb{R}^2)$ . Thus, Campbell's formula (see Theorem 1) yields

$$\mathbb{E} \left( \sum_{\tilde{L}_n \in S_H^*} h(|\tilde{L}_n|) \mid S_H^* \right) = \lambda'_\ell \int_{S_H^*} h(|u|) \nu_1(du)$$

and, for  $h(|u|) = \mathbf{1}_{[0,x]}(|u|)$ , formula (1.16) follows.  $\square$

### 1.4.3.2 Probability density of $D^*$

Using Theorem 13 we can derive analogous representation formulae for the probability density of  $D^*$ .

**Theorem 14.** (i) If  $L$  is a planar Poisson process, which is independent of  $T$  and  $H$ , then the probability density  $f_{D^*} : [0, \infty) \rightarrow [0, \infty)$  of  $D^*$  is given by

$$f_{D^*}(x) = \lambda_\ell \gamma \mathbf{E} v_1(\Xi_H^* \cap \partial B_x(o)), \quad x \geq 0, \quad (1.17)$$

where  $v_1(\Xi_H^* \cap \partial B_x(o))$  denotes the curve length of the circle  $\partial B_x(o)$  inside  $\Xi_H^*$ .

(ii) If  $L$  is a Cox processes on  $T^{(1)}$  which is conditionally independent of  $H$  given  $T$ , then the probability density of  $D^*$  is given by

$$f_{D^*}(x) = \lambda_\ell \mathbf{E} \left( \sum_{i=1}^{N_x^*} \frac{1}{\sin \alpha_i^*} \right), \quad x \geq 0, \quad (1.18)$$

where  $N_x^* = |S_H^* \cap \partial B_x(o)|$  is the number of intersection points of the segment system  $S_H^*$  with  $\partial B_x(o)$  and  $\alpha_1^*, \dots, \alpha_{N_x^*}^*$  are the angles at the corresponding intersection points between their tangents to  $\partial B_x(o)$  and the intersecting segments.

*Proof.* Assuming that  $L$  is a Poisson process and using the polar decomposition of the 2-dimensional Lebesgue measure, we get from (1.15) that

$$\begin{aligned} F_{D^*}(x) &= \lambda_\ell \gamma \mathbf{E} \int_{\mathbb{R}^2} \mathbf{1}_{\Xi_H^* \cap B_x(o)}(y) v_2(dy) \\ &= \lambda_\ell \gamma \mathbf{E} \int_0^x \int_0^{2\pi} r \mathbf{1}_{\Xi_H^*}((r \cos t, r \sin t)) dt dr \\ &= \int_0^x \lambda_\ell \gamma \mathbf{E} v_1(\Xi_H^* \cap \partial B_r(o)) dr, \end{aligned}$$

i.e., (1.17) is shown. If  $L$  is a Cox process on  $T^{(1)}$ , then we get from (1.16) that

$$\begin{aligned} F_{D^*}(x) &= \lambda_\ell \mathbf{E} v_1(S_H^* \cap B_x(o)) \\ &= \lambda_\ell \mathbf{E} \int_0^\infty \sum_{i=1}^{N_y^*} \frac{1}{\sin \alpha_i^*} \mathbf{1}_{[0,x]}(y) dy \\ &= \int_0^x \lambda_\ell \mathbf{E} \left( \sum_{i=1}^{N_y^*} \frac{1}{\sin \alpha_i^*} \right) dy, \end{aligned}$$

decomposing the Hausdorff measure  $v_1$  similarly as in the proof of (1.17).  $\square$

### 1.4.3.3 Representation formulae for $C^*$

**Theorem 15.** Let  $L$  be a Cox processes on  $T^{(1)}$  which is conditionally independent of  $H$  given  $T$ . Then, for any measurable function  $h : \mathbb{R} \rightarrow [0, \infty)$  it holds that

$$\mathbf{E}h(C^*) = \lambda_\ell \mathbf{E} \int_{S_H^*} h(c(y)) v_1(dy), \quad (1.19)$$

where  $c(y)$  is the shortest path length from  $y$  to  $o$  along the edges of the Palm version  $H_S^*$  of  $H_S$  and  $S_H^*$  is the (typical) segment system of  $H_S^*$  centered at  $o$ .

The *proof* of Theorem 15 is similar to the proof of Theorem 13. Note that formula (1.19) can be written as

$$\mathbf{E}h(C^*) = \lambda_\ell \mathbf{E} \sum_{i=1}^N \int_{c(A_i)}^{c(B_i)} h(u) du,$$

where the segment system  $S_H^*$  is decomposed into line segments  $S_1, \dots, S_N$  with endpoints  $A_1, B_1, \dots, A_N, B_N$  such that  $S_H^* = \bigcup_{i=1}^N S_i$ ,  $\nu_1(S_i \cap S_j) = 0$  for  $i \neq j$ , and  $c(A_i) < c(B_i) = C(A_i) + \nu_1(S_i)$ . Furthermore, putting  $h(x) = \mathbf{1}_B(x)$  for any Borel set  $B \subset \mathbb{R}$ , we get that  $\mathbb{P}(C^* \in B) = \int_B \lambda_\ell \mathbf{E} \sum_{i=1}^N \mathbf{1}_{[c(A_i), c(B_i)]}(u) du$ . Thus, the following formulae for the probability density  $f_{C^*} : \mathbb{R} \rightarrow [0, \infty)$  of  $C^*$  are obtained:

$$f_{C^*}(x) = \begin{cases} 2\lambda_\ell & \text{if } x = 0, \\ \lambda_\ell \mathbf{E} \sum_{i=1}^N \mathbf{1}_{[c(A_i), c(B_i)]}(x) & \text{if } x > 0. \end{cases} \quad (1.20)$$

## 1.5 Scaling limits

In this section we assume that  $L$  is a Cox process on  $T^{(1)}$  with random driving measure given by (1.11). We investigate the asymptotic behavior of the distributions of the typical connection lengths  $D^*$  and  $C^*$  as the parameters of the stochastic network model introduced in Section 1.4.2 tend to some extremal values. The resulting limit theorems for the distributions of  $D^*$  and  $C^*$  can be used in order to derive parametric approximation formulae for the distribution of  $C^*$ , see Section 1.6.

### 1.5.1 Asymptotic behavior of $D^*$

We consider the asymptotic behavior of the distribution of  $D^* = D^*(\gamma, \lambda_\ell)$  if the scaling factor  $\kappa = \gamma/\lambda_\ell$  introduced in Section 1.2.2 tends to  $\infty$ , where we assume that  $\gamma \rightarrow \infty$  and  $\lambda_\ell \rightarrow 0$  such that  $\lambda_\ell \gamma = \lambda$  is fixed. This means that the planar intensity  $\lambda$  of  $H$  is constant, but the edge set of  $T_\gamma$  gets unboundedly dense as  $\kappa \rightarrow \infty$ ; see Figure 1.10 for realizations of the network model for extremely small and large values of  $\kappa$ . In particular, we show that  $D^*$  converges in distribution to the (random) Euclidean distance  $Z$  from the origin to the nearest point of a stationary Poisson process in  $\mathbb{R}^2$  with intensity  $\lambda$ .

**Theorem 16.** *Let  $T$  be ergodic and  $Z \sim \text{Wei}(\lambda\pi, 2)$  for some  $\lambda > 0$ . If  $\kappa \rightarrow \infty$ , where  $\gamma \rightarrow \infty$  and  $\lambda_\ell \rightarrow 0$  such that  $\lambda = \gamma\lambda_\ell$ , then*

$$D^*(\gamma, \lambda_\ell) \xrightarrow{d} Z. \quad (1.21)$$

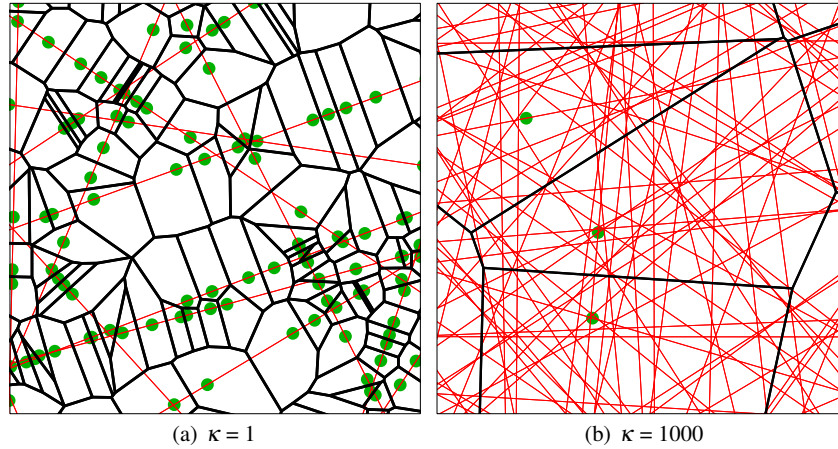


**Fig. 1.10** Realizations of the network model for extreme values of  $\kappa$

In the *proof* of Theorem 16 given below, we use two classical results regarding weak convergence of point processes, which are stated separately in Section 1.5.1.1. For further details on weak convergence of point processes, see e.g. [3, 9, 12].

### 1.5.1.1 Weak convergence of point processes

A sequence of point processes  $X^{(1)}, X^{(2)}, \dots$  in  $\mathbb{R}^2$  is said to *converge weakly* to a point process  $X$  in  $\mathbb{R}^2$  iff

$$\lim_{m \rightarrow \infty} \mathbb{P}(X^{(m)}(B_1) = i_1, \dots, X^{(m)}(B_k) = i_k) = \mathbb{P}(X(B_1) = i_1, \dots, X(B_k) = i_k)$$

for any  $k \geq 1$ ,  $i_1, \dots, i_k \geq 0$  and for any continuity sets  $B_1, \dots, B_k \in \mathcal{B}_0(\mathbb{R}^2)$  of  $X$ , where  $B \in \mathcal{B}(\mathbb{R}^2)$  is called a *continuity set* of  $X$  if  $\mathbb{P}(X(\partial B) > 0) = 0$ . If the sequence  $X^{(1)}, X^{(2)}, \dots$  converges weakly to  $X$ , we briefly write  $X^{(m)} \Longrightarrow X$ .

Now let  $X = \{X_n\}$  be an arbitrary ergodic point process in  $\mathbb{R}^2$  with intensity  $\lambda \in (0, \infty)$ . Then the following limit theorem for independently thinned and appropriately re-scaled versions of  $X$  can be shown. For each  $p \in (0, 1)$ , let  $X^{(p)}$  denote the point process which is obtained from  $X$  by an independent thinning, where each point  $X_n$  of  $X$  survives with probability  $p$  and is removed with probability  $1 - p$  independently of the other points of  $X$ . Furthermore, assume that  $Y^{(p)}$  is a re-scaled version of the thinned process  $X^{(p)}$ , which is defined by  $Y^{(p)}(B) = X^{(p)}(B/\sqrt{p})$  for each  $B \in \mathcal{B}(\mathbb{R}^2)$ . Thus, for each  $p \in (0, 1)$ , the point processes  $Y^{(p)}$  and  $X$  are both stationary with the same intensity  $\lambda$  since  $\mathbf{E}Y^{(p)}([0, 1]^2) = \mathbf{E}X^{(p)}([0, 1/\sqrt{p}]^2) = \lambda$ .

**Theorem 17.** *Let  $Y$  be a stationary Poisson process in  $\mathbb{R}^2$  with intensity  $\lambda$ . Then,*

$$Y^{(p)} \Longrightarrow Y \quad \text{as } p \rightarrow 0. \quad (1.22)$$

For a *proof* of this result, see e.g. Section 11.3 of [3] or Theorem 7.3.1 in [12].

Intuitively, the statement of Theorem 1.22 can be explained as follows. The dependence between the points of  $X$  in two sets  $A, B \in \mathcal{B}_0(\mathbb{R}^2)$  decreases with increasing distance between  $A$  and  $B$ . Thus, if the point process is thinned independently only points far away of each other survive with high probability which in the limit yields a point process with complete spatial randomness, that is a Poisson process.

The following continuity property with respect to weak convergence of Palm distributions of stationary point processes holds.

**Theorem 18.** *Let  $X, X^{(1)}, X^{(2)}, \dots$  be stationary point processes in  $\mathbb{R}^2$  with intensities  $\lambda, \lambda_1, \lambda_2, \dots$ , respectively. If  $\lambda_m = \lambda$  for all  $m \geq 1$  and in addition  $X^{(m)} \implies X$  as  $m \rightarrow \infty$ , then the Palm versions  $X^{(1)*}, X^{(2)*}, \dots$  of  $X^{(1)}, X^{(2)}, \dots$  converge weakly to the Palm version  $X^*$  of  $X$ , i.e.,*

$$X^{(m)*} \implies X^* \quad \text{as } m \rightarrow \infty. \quad (1.23)$$

For a *proof* of Theorem 18, see e.g. Proposition 10.3.6 in [12].

### 1.5.1.2 Proof of Theorem 16

We now are able to prove Theorem 16 using the auxiliary results stated above, where we first show that the Cox process  $H$  on  $T^{(1)}$  converges weakly to a stationary Poisson process with intensity  $\lambda$  if  $\kappa \rightarrow \infty$  provided that  $\lambda_\ell \gamma = \lambda$  is constant. This result is then used in order to investigate the asymptotic behavior of the typical Euclidean distance  $D^* = |\tilde{H}_0|$ , where  $\tilde{H}_0$  denotes that point of  $\tilde{H} = \{\tilde{H}_n\}$  which is closest to the origin (see Section 1.4.2.2).

**Lemma 1.** *If  $\kappa = \gamma/\lambda_\ell \rightarrow \infty$ , where  $\lambda_\ell \gamma = \lambda$  for some constant  $\lambda \in (0, \infty)$ , then  $H \implies Y$ , where  $Y$  is a stationary Poisson process in  $\mathbb{R}^2$  with intensity  $\lambda$ .*

*Proof.* For each  $\gamma > 1$ , let  $H = H(\gamma)$  be the Cox process on the scaled version  $T_\gamma$  of  $T$  with linear intensity  $\lambda_\ell$ , where  $\lambda_\ell = \lambda/\gamma$  for some constant  $\lambda \in (0, \infty)$ . Then the Cox process  $H(\gamma)$  can be obtained from  $H(1)$  by an independent thinning with survival probability  $p = 1/\gamma$  followed by a re-scaling with the scaling factor  $\sqrt{1/\gamma}$ , i.e.,  $H(\gamma) \stackrel{d}{=} H(1)^{(p)}$ . Furthermore, the Cox process  $H(1)$  is ergodic since the underlying tessellation  $T$  and hence the random intensity measure of  $H(1)$  is ergodic. Thus we can apply Theorem 17 which yields  $H(\gamma) \implies Y$  as  $\gamma \rightarrow \infty$ .  $\square$

**Lemma 2.** *Let  $Z \sim \text{Wei}(\lambda\pi, 2)$  for some  $\lambda > 0$ . Then  $D^* \xrightarrow{d} Z$  as  $\kappa \rightarrow \infty$  provided that  $\gamma \rightarrow \infty$  and  $\lambda_\ell \rightarrow 0$  such that  $\lambda_\ell \gamma = \lambda$ .*

*Proof.* Assume that  $H^* = H^*(\gamma)$  is the Palm version of the stationary point process  $H = H(\gamma)$ . Furthermore, assume that  $Y$  is a stationary Poisson process in  $\mathbb{R}^2$  with intensity  $\lambda$ . Then the distribution of  $Y \cup \{o\}$  is equal to the Palm distribution of  $Y$  due to Slivnyak's theorem. Thus, Lemma 1 and Theorem 18 yield that

$$H^*(\gamma) \implies Y \cup \{o\} \quad (1.24)$$

if  $\gamma \rightarrow \infty$  and  $\lambda_\ell \rightarrow 0$  with  $\lambda_\ell \gamma = \lambda$ . Since both  $L$  and  $H$  are Cox processes on  $T_\gamma^{(1)}$  conditionally independent given  $T_\gamma$ , we get that  $\tilde{H} \cup \{o\}$  and the Palm version  $H^*$  of  $H$  have the same distributions. This is a consequence of Slivnyak' theorem for stationary Cox processes, see Theorem 8. Thus, using (1.24), for each  $r > 0$  we get

$$\begin{aligned} \lim_{\gamma \rightarrow \infty} \mathbb{P}(|\tilde{H}_0| > r) &= \lim_{\gamma \rightarrow \infty} \mathbb{P}(\tilde{H}(B_r(o)) = 0) \\ &= \lim_{\gamma \rightarrow \infty} \mathbb{P}((\tilde{H} \cup \{o\})(B_r(o)) = 1) \\ &= \lim_{\gamma \rightarrow \infty} \mathbb{P}(H^*(B_r(o)) = 1) \\ &= \mathbb{P}((Y \cup \{o\})(B_r(o)) = 1) \\ &= \mathbb{P}(Y(B_r(o)) = 0). \end{aligned}$$

Hence,  $\lim_{\gamma \rightarrow \infty} \mathbb{P}(|\tilde{H}_0| > r) = \mathbb{P}(Y(B_r(o)) = 0) = \exp(-\lambda \pi r^2)$  for each  $r > 0$ , which shows that  $D^* = |\tilde{H}_0| \stackrel{d}{\rightarrow} Z \sim \text{Wei}(\lambda \pi, 2)$ .  $\square$

### 1.5.2 Asymptotic behavior of $C^*$

The results presented in the preceding section can be extended to further cost functionals of the stochastic network model introduced in Section 1.4.2. For instance, if  $T$  is isotropic, mixing and  $\mathbf{E}v_1^2(\partial \Xi^*) < \infty$ , where  $v_1^2(\partial \Xi^*)$  denotes the circumference of the typical cell  $\Xi^*$  of  $T$ , then it can be shown that

$$C^* \stackrel{d}{\rightarrow} \xi Z \quad (1.25)$$

as  $\kappa = \gamma/\lambda_\ell \rightarrow \infty$  provided that  $\lambda = \gamma\lambda_\ell$  is fixed. Here,  $Z \sim \text{Wei}(\lambda \pi, 2)$  and  $\xi \in [1, \infty)$  is some constant which depends on type of the underlying tessellation  $T$ . In the proof of (1.25), the result of Theorem 16 is used. This is then combined with fact that under the additional conditions on  $T$  mentioned above, one can show that  $C^* - \xi D^*$  converges in probability to 0. Moreover, it can be shown that

$$C^* \stackrel{d}{\rightarrow} Z' \quad (1.26)$$

as  $\kappa = \gamma/\lambda_\ell \rightarrow 0$ , where  $\lambda_\ell$  is fixed and  $Z' \sim \text{Exp}(2\lambda_\ell)$ . For further details, see [20].

## 1.6 Monte Carlo methods and parametric approximations

The representation formulae (1.15) – (1.17) can easily be used to obtain simulation-based approximations for the distribution function and probability density of  $D^*$ ,

see Section 1.6.1. These estimates can be computed based on samples of  $\Xi_H^*$  and  $S_H^*$  which are generated by Monte Carlo simulation, using algorithms like those discussed in Section 1.3.2.2. Note that we do not have to simulate any points of  $L$ .

Similarly, we can use formula (1.20) to get a Monte Carlo estimator for the density of  $C^*$ . However, note that the density formula (1.18) for  $D^*$  is not suitable in this context, because it would lead to an estimator which is numerically instable.

Moreover, the scaling limits for  $C^*$  stated in (1.25) and (1.26) can be used in order to determine parametric approximation formulae for the density of  $C^*$ , which are surprisingly accurate for a wide range of (non-extremal) model parameters, see Section 1.6.2.

### 1.6.1 Simulation-based estimators

Assume that  $\Xi_{H,1}^*, \dots, \Xi_{H,n}^*$  and  $S_{H,1}^*, \dots, S_{H,n}^*$  are  $n$  independent copies of  $\Xi_H^*$  and  $S_H^*$ , respectively. If  $L$  is a stationary Poisson process in  $\mathbb{R}^2$ , then we can use (1.15) and (1.17) to define the estimators for  $F_{D^*}(x)$  and  $f_{D^*}(x)$  by

$$\widehat{F}_{D^*}(x; n) = \frac{\lambda_\ell \gamma}{n} \sum_{i=1}^n \nu_2(\Xi_{H,i}^* \cap B_x(o)) \quad (1.27)$$

and

$$\widehat{f}_{D^*}(x; n) = \frac{\lambda_\ell \gamma}{n} \sum_{i=1}^n \nu_1(\Xi_{H,i}^* \cap \partial B_x(o)), \quad (1.28)$$

respectively. If  $L$  is a Cox process on  $T^{(1)}$ , then we can use (1.16) to define an estimator for  $F_{D^*}(x)$  by

$$\widehat{F}_{D^*}(x; n) = \frac{\lambda_\ell}{n} \sum_{i=1}^n \nu_1(S_{H,i}^* \cap B_x(o)). \quad (1.29)$$

Similarly, using formula (1.20), we can define an estimator for  $f_{C^*}(x)$  by

$$\widehat{f}_{C^*}(x; n) = \frac{\lambda_\ell}{n} \sum_{j=1}^n \sum_{i=1}^{N_j} \mathbf{1}_{[c(A_i^{(j)}), c(B_i^{(j)})]}(x), \quad (1.30)$$

where the independent copies  $S_{H,1}^*, \dots, S_{H,n}^*$  of  $S_H^*$  are decomposed into the line segments  $S_1^{(j)}, \dots, S_{N_j}^{(j)}$  with endpoints  $A_1^{(j)}, B_1^{(j)}, \dots, A_{N_j}^{(j)}, B_{N_j}^{(j)}$ . It is not difficult to see that the estimators given in (1.27)–(1.30) are unbiased and in addition strongly consistent for fixed  $x \geq 0$ . However, if  $L$  is a Cox process, then it is not recommended to construct an estimator  $\widehat{f}_{D^*}(x; n)$  for  $f_{D^*}(x)$  based on equation (1.18) by just omitting the expectation in (1.18). This estimator is numerically unstable since infinitely small angles can occur. In this case, it is better to first compute the distribution function  $\widehat{F}_{D^*}(x; n)$  using formula (1.29) and afterwards considering difference quotients obtained from this estimated distribution function as estimator  $\widehat{f}_{D^*}(x; n)$  for  $f_{D^*}(x)$ , see [21]. Some examples of estimated densities are shown in Figures 1.11 and 1.12,

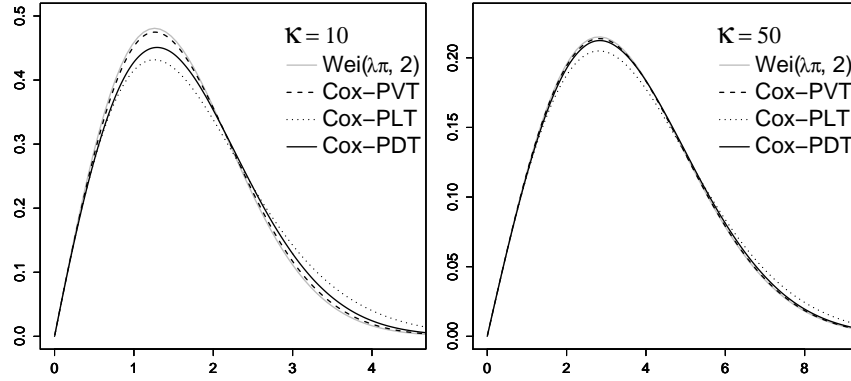


**Fig. 1.11** Estimated density of  $D^*$  if  $L$  is a stationary Poisson process in  $\mathbb{R}^2$

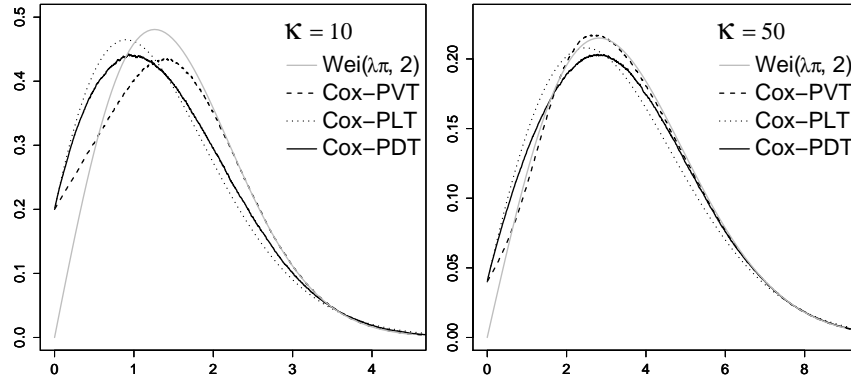


**Fig. 1.12** Estimated density of  $D^*$  if  $L$  is a Cox process on  $T^{(1)}$

together with the corresponding (scaling) limit as  $\kappa = \gamma/\lambda_\ell \rightarrow \infty$  with  $\lambda_\ell \gamma (= \lambda)$  fixed., i.e. the density of the  $\text{Wei}(\lambda \pi, 2)$ -distribution.

### 1.6.2 Parametric approximation formulae

For practical applications it is useful to have parametric approximation formulae for the distribution of  $C^*$ , where the parameters depend on the model type of  $T$  and the scaling factor  $\kappa$ . Therefore, the problem arises to fit suitable classes of parametric densities to the densities of  $C^*$  which have been computed by the simulation-based algorithm discussed in Section 1.6.1. In [7] truncated Weibull distributions were used for this purpose since the scaling limits for the distribution of  $C^*$ , i.e. the exponential and Weibull distributions mentioned in Section 1.5.2, belong to this

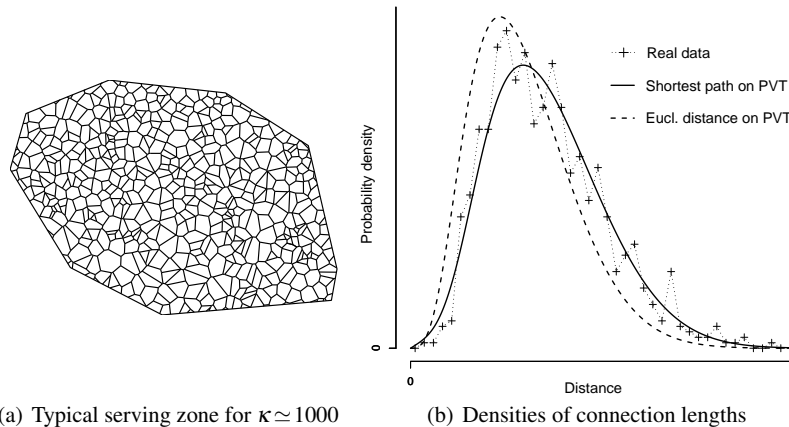


**Fig. 1.13** (a) Typical serving zone for  $\kappa = 1000$  and (b) parametric density of  $C^*$  for PVT fitted to infrastructure data (solid line), compared to histogram of connection lengths estimated from real network data, showing that the assumption of direct physical connections (dashed line) is incorrect.

parametric family. It turned out that the fitted densities approximate the estimated densities surprisingly well for different types of  $T$  and for a wide range of  $\kappa$ . These parametric densities can be used in order to efficiently analyze and plan telecommunication networks. In a first step, a suitable tessellation model has to be fitted to real infrastructure data. Afterwards, the scaling factor  $\kappa$  must be estimated computing length intensity of the infrastructure and the number of HLC in the network per unit area. Then the distribution of the typical shortest path length  $C^*$  is directly available via the parametric densities in order to analyze connection lengths of existing or planned telecommunication networks. In Figure 1.13 the parametric density chosen in this way is compared to a histogram of connection lengths of real network data of Paris. One can see that there is a quite good fit, see [7] for details and further results.

## References

1. F. Baccelli and B. Blaszczyzyn *Stochastic Geometry and Wireless Networks*. NOW Publishers, Delft 2009.
2. R. Cowan. Properties of ergodic random mosaic processes. *Mathematische Nachrichten*, 97:89–102, 1980.
3. D.J. Daley and D. Vere-Jones. *An Introduction to the Theory of Point Processes*, volume I and II. Springer, New York, 2005/2008.
4. F. Fleischer, C. Gloaguen, H. Schmidt, V. Schmidt, and F. Schweiggert. Simulation algorithm of typical modulated Poisson-Voronoi cells and application to telecommunication network modelling. *Japan Journal of Industrial and Applied Mathematics*, 25(3):305–330, 2008.
5. F. Fleischer, C. Gloaguen, V. Schmidt, and F. Voss. Simulation of the typical Poisson-Voronoi-Cox-Voronoi cell. *Journal of Statistical Computation and Simulation*, 79(7):939–957, 2009.

6. C. Gloaguen, F. Fleischer, H. Schmidt, and V. Schmidt. Simulation of typical Cox-Voronoi cells, with a special regard to implementation tests. *Mathematical Methods of Operations Research*, 62:357–373, 2005.
7. C. Gloaguen, F. Voss, and V. Schmidt. Parametric distance distributions for fixed access network analysis and planning. In *Proceedings of the 21st International Teletraffic Congress*, Paris, France, September 2009.
8. M. Haenggi, J. G. Andrews, F. Baccelli, O. Dousse and M. Franceschetti. Stochastic geometry and random graphs for the analysis and design of wireless networks. *IEEE Journal on Selected Areas in Communications*, 27:1029–1046, 2009.
9. O. Kallenberg. *Random Measures*. Akademie-Verlag, Berlin, 4th edition, 1986.
10. C. Lautensack and S. Zuyev. Random Laguerre tessellations. *Advances in Applied Probability*, 40:630–650, 2008.
11. R. Maier, J. Mayer, and V. Schmidt. Distributional properties of the typical cell of stationary iterated tessellations. *Mathematical Methods of Operations Research*, 59:287–302, 2004.
12. K. Matthes, J. Kerstan, and J. Mecke. *Infinitely Divisible Point Processes*. J. Wiley & Sons, Chichester, 1978.
13. J. Mecke. Parametric representation of mean values for stationary random mosaics. *Mathematische Operationsforschung und Statistik*, 12:437–442, 1984.
14. J. Neveu. Sur les mesures de Palm de deux processus ponctuels stationnaires. *Zeitschrift für Wahrscheinlichkeitstheorie und verwandte Gebiete*, 34:199–203, 1976.
15. M. P. Quine and D. F. Watson. Radial generation of n-dimensional Poisson processes. *Journal of Applied Probability*, 21:548–557, 1984.
16. R. Schneider and W. Weil. *Stochastic and Integral Geometry*. Springer, Berlin, 2008.
17. D. Stoyan, W. S. Kendall, and J. Mecke. *Stochastic Geometry and its Applications*. J. Wiley & Sons, Chichester, second edition, 1995.
18. K. Tchoumatchenko and S. Zuyev. Aggregated and fractal tessellations. *Probability Theory Related Fields*, 121:198–218, 2001.
19. F. Voss, C. Gloaguen, F. Fleischer, and V. Schmidt. Distributional properties of Euclidean distances in wireless networks involving road systems. *IEEE Journal on Selected Areas in Communications*, 27:1047–1055, 2009.
20. F. Voss, C. Gloaguen, and V. Schmidt. Scaling limits for shortest path lengths along the edges of stationary tessellations. *Preprint*, 2009.
21. F. Voss, C. Gloaguen, F. Fleischer, and V. Schmidt. Densities of shortest path lengths in spatial stochastic networks. *Preprint*, 2009.
22. S. Zuyev. Stochastic geometry and telecommunication networks. In W. S. Kendall and I. Molchanov, editors, *New Perspectives in Stochastic Geometry*, Oxford University Press, Oxford 2009.